

# CHALMERS



## Boundary element method for intensity potential approach - Evaluation of a tool for prediction of high-frequency noise radiation from engine bays

*Master's Thesis 2010:99*

NATA AMIRYARAHMADI

*Department of Civil and Environmental Engineering  
Division of Applied Acoustics  
Vibroacoustics Group*

CHALMERS UNIVERSITY OF TECHNOLOGY  
Göteborg, Sweden 2010



MASTER'S THESIS 2010:99

Boundary element method for intensity potential  
approach - Evaluation of a tool for prediction of  
high-frequency noise radiation from engine bays

Nata Amiryarahmadi

Department of Civil and Environmental Engineering  
*Division of Applied Acoustics*  
*Vibroacoustics Group*  
CHALMERS UNIVERSITY OF TECHNOLOGY  
Göteborg, Sweden 2010

Boundary element method for intensity potential approach-Evaluation of a tool for prediction of high-frequency noise radiation from engine bays

© Nata Amiryarahmadi, 2010

Master's Thesis 2010:99

Department of Civil and Environmental Engineering  
Division of Applied Acoustics  
Vibroacoustics Group  
Chalmers University of Technology  
SE-41296 Göteborg  
Sweden

Tel. +46-(0)31 772 1000

Reproservice / Department of Civil and Environmental Engineering  
Göteborg, Sweden 2010

Boundary element method for intensity potential approach - evaluation of a tool for prediction of high-frequency noise radiation from engine bays

Nata Amiryarahmadi

Department of Civil and Environmental Engineering

Division of Applied Acoustics

Vibroacoustics Group

Chalmers University of Technology

## Abstract

Motor vehicles are identified as a main source of excessive noise in urban areas. This has motivated many governments to set strict regulations to force automotive industries in order to control noise levels in their products. Fulfilling these regulations demands investing lots of time and money on noise reduction research. Current thesis is part of the research that Applied Acoustics at Chalmers and Saab Automobile AB started together with KTH entitled "Reduction of external noise for diesel propelled passenger cars".

This study aims to predict sound radiation from engine bay at high frequencies (1-10 kHz) using a computer model called BEMIPA. This model applies boundary element method (BEM) to an energy-based method called Intensity Potential Approach (IPA) which applies Helmholtz decomposition theorem to predict the active intensity vector. BEMIPA calculates time-averaged energy transfer functions radiated to the receiver points. During the project, sound radiation from different geometry configurations of the engine bay is calculated. To reduce complexity and time of the calculations, geometry models are simplified by neglecting many details such as cables and pipes. The model is evaluated by comparing the calculation results with measurements taken from three engine bays with similar geometry. The finalized model can later be used to find optimum modifications required to come up with quieter engine bays.

Calculation results show that when BEMIPA is used to predict total sound radiation from several sources in a region, the difference between simulation and measurement results does not exceed 4dB and there is also a good agreement between the trend of calculated and measured radiation curves. Investigation on absorbers proves that assigning proper absorption coefficient to the right surfaces of the model, is a determining factor to achieve a satisfactory prediction of the high frequency sound field. In addition, the results show that although the effect of scattering objects such as pipes and cables cannot be totally neglected, but it can be replaced by assigning proper equivalent scattering absorption properties to the surfaces inside the engine bay.

Analyzing the calculation results and comparing them with the measurements proves that BEMIPA method is an efficient tool for prediction of high-frequency sound field radiated from a complex geometry such as an engine bay. Although this method is not capable of showing resonances and other details of the radiated field, but it is a strong tool to predict the general behaviour of the radiation at high frequencies.

**Key words:** BEM (Boundary Element Method), Intensity Potential Approach, Helmholtz decomposition theorem, equivalent scattering absorption.



## Acknowledgements

This thesis is carried out as a part of project “Reduction of external noise for diesel propelled passenger cars”, sponsored by EMFO (Dnr AL 90B2004:156660) and Vinnova/Green Car (Dnr 2005-00059) and conducted by Applied Acoustic at Chalmers University of Technology, Saab Automobile AB and KTH.

I would like to express my deepest gratitude to Patrik Andersson, my very responsible, helpful and knowledgeable supervisor. His patience and understanding during the project gave me the great feeling of confidence and his creative ideas besides his excellent supervision made this thesis more challenging and attractive to me.

My special thanks to Wolfgang Kropp who is and will always be a great teacher for me. His perfect administration in Technical Acoustics has made this department a very pleasant second-home for all the students.

I am endlessly grateful to my kind, loving and supportive family; my dearest parents, my sweet sister and my gorgeous grandmother. I would like you to know that no matter how far I am from you now, your love and belief in me is the only power that gives me the strength to conquer my fears, stand on my feet and continue the path to fulfil my dreams.

My heartily appreciation to my dearest Emad for always being there for me and replacing the sorrow of homesickness with the most joyful and pleasant moments of life. Thank you for sharing all these laughter with me and holding me up when I feel down.

Last but not the least, thousands of thanks to kind Gunilla Skog and Börje Wijk and to my dear teachers Mendel Kleiner, Daniel Västfjäll, Tor Kihlman, Krister Larsson and all the PhD students at Applied Acoustics whose educational supports as well as their friendliness made studying at Technical Acoustics department quite a pleasure for me.





# Contents

1. Introduction.....	1
2. Theory.....	3
2.1. IPA .....	3
2.2. BEM.....	5
2.3. 3D models .....	7
2.4. Scattering objects .....	9
2.5. Model of absorbers .....	10
3. Measurements .....	13
4. Calculations .....	15
4.1. Selected source positions for calculations.....	15
5. Results: Understanding the acoustic behaviour of BEMIPA..	18
5.1. Investigation on different geometry models .....	19
5.1.1. Simplified geometries .....	19
5.1.2. Detailed geometry .....	21
5.1.3. Comparing the results of different geometry models .....	23
5.2. Modelling and measurement differences.....	24
5.3. Absorption effect .....	25
5.3.1. Effect of ideal absorber on all surfaces .....	27
5.3.2. Effect of using ideal absorber on the main absorbers.....	28
5.3.3. Effect of the equivalent scattering absorbers .....	29
6. Results: Prediction of the radiated sound field from an engine bay.....	31
6.1. Total averaged radiated power from several sources.....	31
7. Conclusions .....	34
7.1. Summary.....	34

7.2. Outcome of the thesis.....	35
7.3. Future work.....	36
Bibliography .....	37
Appendix A .....	38
A.1.Simplified model without the back part .....	38
A.2.Effect of the back part .....	39
A.3. Detailed model calculations.....	40
A.4. Effect of ideal absorber on all surfaces .....	41
A.5. Effect of using ideal absorber on the main absorbers .....	42
A.6. Effect of equivalent scattering absorbers .....	43
Appendix B .....	44
Radiated power from sources close to absorbers.....	44



# 1. Introduction

Motor vehicles as the main source of urban noise have attracted very much attention among the developed countries during the recent years. The European Union (EU) has been one of the pioneers to bring its environmental concerns about the increase of pollution due to the cars into action. EU has set some strict regulations in different areas to control the polluting effects of the vehicles. These regulations are listed and explained in the Directives of EU [1]. Parallel to the European emission standard which defines the acceptable limits for exhaust gas emissions of new vehicles, the directives state the noise level limits for all the vehicles produced, sold or used in the EU. Based on the EU Legislations published in their website, for any motor vehicle intended for use on the road, with or without bodywork, having at least four wheels and a maximum design speed exceeding 25 km/h, the noise level limits range from 74 dB(A) for motor cars to 80 dB(A) for high-powered goods vehicles. These limits are set for mechanical parts and exhaust systems of the vehicles. [1]

The new regulations in EURO regarding environmental issues demands the reduction of CO<sub>2</sub> level in exhaust gases, also global concerns about the shortage and high prices of fossil fuels in the near future makes the car manufacturers decrease the energy consumption of their cars. One solution to fulfil both of these requirements to some extent in diesel engines is to increase the compression rate of the cylinder and shorten the combustion time. Like many other solutions in the world of technology this method has disadvantages as well one of which is the increase of the engine noise with high frequency content.

Applied Acoustics at Chalmers has been conducting a research entitled "Reduction of external noise for diesel propelled passenger cars" with Saab Automobile AB and KTH to investigate on the solutions to decrease the exterior noise. A long term goal of this part of the research is to investigate the noise emission from the engine bay at high frequencies (1-10 kHz), formulate it and come up with some solutions to reduce the noise by modifying the absorption properties of different surfaces in the engine bay. This thesis is an early step to gain general knowledge about the high-frequency acoustical behaviour of engine bays. Moreover, to reach the long term goals of the project, in this thesis a computer model called BEMIPA is used as a tool to predict and optimize the acoustical performance of the engine bay. The model is evaluated during the project by comparing the calculated results with the measurements. Through the evaluations it is investigated how assigned boundary conditions (absorption) affect the results. It is also studied whether or not in simplified models

of engine bay the effect of accessory parts, causing scattering of sound, can be replaced and approximated by additional wall absorption.

Engine bay is a construction with complex geometry, many openings and full of accessory parts. To model such a complex geometry using numerical computation methods such as the finite element method (FEM) or the boundary element method (BEM) seem more appropriate. These methods discretize the complex system to small elements and form partial differential equations (PDE) for each element; by assuming proper boundary conditions, partial differential equation system can be solved and the required parameters such as sound power levels at any position of the domain can be obtained. However, when modelling the sound radiation at high frequencies, classical FEM for the Helmholtz equation (H-FEM) or BEM for the Kirchhoff-Helmholtz integral equation (KH-BEM) are not suitable choices to solve the problem. In these classical approaches element size varies with frequency and by increasing frequency the required element size becomes smaller. Therefore, modelling a complex system with a large domain such as an engine bay would demand excessive number of elements resulting in too costly and time consuming calculations. In addition, when the frequency increases and wave lengths become smaller, the required accuracy of the geometry model and boundary conditions increase accordingly and the results become hyper-sensitive to the geometry, boundary conditions and environmental conditions.

At high frequencies looking for the exact response at one point or a specific frequency is quite unreasonable due to the uncertainties of the model which can give quite different results even for identical objects. Instead, the methods based on spatial, frequency and ensemble averages of energy or kinetic variables are more appropriate. These methods can predict the general behaviour of many similar individuals and in that case can fulfil the aim of this thesis which is predicting sound radiation from engine bays with the same design but having difference in details. One of these energy-based methods which is used in this project is called Intensity Potential Approach (IPA) that was developed by Thivant and Guyader for cases including an exterior unbounded domain [2]. Intensity potential approach is based on the local energy balance in a lossless medium and Helmholtz decomposition of the vector field of time-averaged sound intensity. The result is a Poisson equation for a scalar intensity potential.

The combination of BEM and IPA methods called as BEMIPA is used to calculate the radiated sound power from the monopole sources in the engine bay. To validate the method, the resulting curves for different geometrical models are compared with the measured radiated power values for three engine bays manufactured by Saab Automobile AB. These calculated data are also the base for deciding about the absorbers effects on the sound radiation from the engine bays.

## 2. Theory

To predict the sound power radiation at high frequencies in this project the boundary element method is applied to the intensity potential approach to solve the power equations at the boundaries of the system.

Following sections take a quick glance at intensity potential approach to model the sound radiation from different source positions in the engine bay as well as the boundary element method and its application in the present project.

### 2.1. IPA

The Intensity Potential Approach, like other energy methods which are developed to predict sound and vibration, is particularly suitable at middle and high frequencies. Because at these frequencies deterministic methods have limitations but instead the assumption of diffuse field and decorrelation become reasonable. All the methods for calculation of vibroacoustic energy flow are based on conservation of energy:

$$\frac{\partial e(r, t)}{\partial t} + \nabla \cdot I(r, t) + \Pi_{dis}(r, t) = \Pi_{in}(r, t) \quad (2.1)$$

where  $e(r, t)$  is the vibration energy at point  $r$  and the time  $t$ .  $I(r, t)$  is the intensity vector,  $\nabla \cdot I(r, t)$  is the divergence of the energy flow and  $\Pi_{dis}(r, t)$  and  $\Pi_{in}(r, t)$  are the density of injected and dissipated energy at  $r$  respectively. For stationary problems the first term is zero and time dependence in other terms disappears.  $\Pi_{dis}(r, t)$  is related to dissipation in the volume which in many practical applications is very small compared to the absorption at the boundaries, so volume dissipation is assumed insignificant and negligible.

Thus, for stationary field:

$$\nabla \cdot I(r) = \Pi_{in}(r) \quad (2.2)$$

$I(r)$ , which is obtained from the average of instantaneous intensity is called active intensity vector.  $\nabla \cdot I(r)$  is the divergence of the active intensity and  $\Pi_{in}(r)$  is the volume density of sound power sources as a function of position  $r$ .

According to Helmholtz decomposition theorem, any continuous vector field whose divergence and curl vanishes at infinity can be decomposed to a curl-free and a divergence-free part. In absence of sound sources at infinity this theorem applies to acoustic active intensity. In other words the acoustic field can be written as the sum of gradient of a scalar potential  $I_\phi(r)$  and the curl of a vector potential  $I_c(r)$ .

$$I(r) = I_\phi(r) + I_C(r) = -\nabla\phi(r) + \nabla \times C(r) \quad (2.3)$$

Irrotational intensity which can be expressed as a scalar potential is enough to describe the flow of acoustic energy, according to Pascal, 1985 [5]. On the other hand the rotational intensity described by a vector potential is responsible for variations in the active intensity field caused by energy vortices, alternated flows of energy or short-circuited energy whose streamlines return to acoustic sources. The net flow of rotational intensity is zero through any closed area [3].

Based on Pascal and Li's investigation [5], the irrotational component has little variation in space and follows geometrical divergence imposed by local energy balance and boundary conditions. The rotational component of intensity is related to effects of interference between waves and usually changes largely in space and frequency. It can be locally added to or subtracted from the irrotational intensity which gives the directivity of total active intensity field. Rotational component does not affect the global power balance. Consequently when the spatial or frequency averages are of interest, neglecting the rotational part is reasonable in many cases. Concluding from the explanations and using equations (2.2) and (2.3), Poisson's equation for sound intensity potential can be resulted:

$$-\Delta\phi(r) = \Pi_{in}(r) \quad (2.4)$$

Equation (2.4) is the fundamental equation for the intensity potential that can be solved by applying boundary element method. This equation is identical to the equation which defines temperature distribution of heat conduction for steady state problems in isotropic media.

IPA can give the total power  $P_{tot}$  radiated through any closed surface  $\Gamma'$  enclosing a volume  $\Omega' \subseteq \Omega$  by integration over the gradient of scalar intensity potential:

$$\begin{aligned} P_{tot} &= \oiint_{\Gamma'} I(r') \cdot d\Gamma(r') \\ &= \oiint_{\Gamma'} (-\nabla\phi(r') + \nabla \times C(r')) \cdot d\Gamma(r') \\ &= \oiint_{\Omega'} \nabla \cdot (-\nabla\phi(r') + \nabla \times C(r')) d\Omega(r') \\ &= \oiint_{\Omega'} \nabla \cdot (-\nabla\phi(r')) d\Omega(r') \\ &= \oiint_{\Gamma'} (-\nabla\phi(r')) \cdot d\Gamma(r') \end{aligned} \quad (2.5)$$

The integration can be made over a surface enclosing the objects and sources in the field or over all openings in the case of radiation from the interior of a partial enclosure.

## 2.2. BEM

The boundary element method, like FEM is a numerical method to solve partial differential equations (PDEs) which have been formulated as integral equations in form of a boundary integral. To model an acoustic system with BEM, the boundaries of the system should be modelled with layers of monopole and dipole power sources. In this case the effect of reflecting and absorbing surfaces is replaced by sources and it resembles the situation of many sources radiating in free field. Based on the boundary conditions of the system and the approach that is used to model the acoustic field, each source should be tuned to give the correct intensity potential and its gradients. Although in many acoustic problems BEM is used to solve Helmholtz equation, but IPA method presented here is based on Poisson's equation which is applied as the governing equation with BEM to model the acoustic field.

The application of BEM to solve the potential problem formulated by IPA is called BEMIPA in the current project. In this method the Poisson's equation is reformulated in integral form:

$$\begin{aligned}
c(r)\phi(r) = & \oint_{\Omega} \Pi_{in}(r')G(r',r)d\Omega(r') \\
& + \oint_{\Gamma} \frac{\partial\phi(r')}{\partial n(r')}G(r',r)d\Gamma(r') \\
& - \oint_{\Gamma} \phi(r')\frac{\partial G(r',r)}{\partial n(r')}d\Gamma(r')
\end{aligned} \tag{2.6}$$

where  $c(r) = \frac{\alpha}{4\pi}$  and  $\alpha$  is the solid angle of the domain  $\Omega$  at point  $r$ .  $c(r)$  is 1 for the points inside the domain, it is  $\frac{1}{2}$  on smooth parts of the boundary and 0 for the points outside the domain. Green's function for Poisson's equation is:

$$G(r',r) = \frac{1}{4\pi R} \tag{2.7}$$

where  $R = \|r - r'\|$  is the distance between points  $r$  and  $r'$  in the domain.

The first term on the right hand side of equation (2.6) describes the direct field from power sources in the domain. Green's function in the second term represents the potential of an omnidirectional power source and the third term of equation (2.6) shows the characteristics of a dipole power source.

Applying proper boundary conditions is required to obtain correct acoustic intensity potential distribution. The boundary should be divided into three categories in a way



that one type of boundary condition applies for each category. The first category is the parts of boundary with input intensity called as  $\Gamma_{in}$ , the second type of boundaries are boundaries with reflecting surfaces called as  $\Gamma_0$  and the last type are those with absorbing surfaces named as  $\Gamma_\alpha$ . Detailed definition of the boundary conditions is presented in [2]. Here, only the formulae which are used to introduce correct boundary conditions to the model are presented:

The power injection at the boundary is formulated using irrotational intensity definition:

$$\frac{\partial \phi(r)}{\partial n(r)} = -I_{in}(r) \quad \forall r \in \Gamma_{in} \quad (2.8)$$

Reflecting surfaces are defined based on the assumption that they do not allow power flow over the boundary:

$$\frac{\partial \phi(r)}{\partial n(r)} = 0 \quad \forall r \in \Gamma_0 \quad (2.9)$$

Deriving the equation for absorbing surfaces was performed by Thivant and Guyader based on the assumption of a local relation between the intensity absorbed by the walls and the intensity potential [2]:

$$\frac{\partial \phi(r)}{\partial n(r)} = -\langle \varepsilon(r, \theta) \rangle_\theta g(r) \phi(r) \quad \forall r \in \Gamma_\alpha \quad (2.10)$$

where  $\langle \varepsilon(r, \theta) \rangle_\theta$  is a function of absorption coefficient of the surface and  $g(r)$  is a pre-calculated function that can be described as the intensity potential on the boundary for the case that all surfaces are acoustically rigid and there is a unit input power.

$\varepsilon(r, \theta)$  has a direct relation with the power absorption coefficient:

$$\varepsilon(r, \theta) = \frac{\alpha(r, \theta)}{2 - \alpha(r, \theta)} 2\pi \cos(\theta) \quad (2.11)$$

Where  $\theta$  is the angle between the normal of the surface at point  $r$  on the boundary and the vector drawn from the source to the point  $r$ . Assuming that the sources are distributed uniformly in a half sphere above the surface, equation (2.12) can be obtained for the diffuse field by integration over the angle  $\theta$ :

$$\langle \varepsilon(r, \theta) \rangle_\theta = \int_0^{\pi/2} \varepsilon(r, \theta) \sin(\theta) d\theta \quad (2.12)$$

After applying the mentioned boundary conditions, the boundary should be discretized into  $N$  elements having surface  $\Gamma_j$  so that the boundary can be defined as:

$$\Gamma \approx \bigcup_{j=1}^N \Gamma_j \quad (2.13)$$

BEMIPA implementation assumes constant potential over each element. The elements have flat triangular shape and collocation points are in the centre of each element.

The boundary element formulation can be written as:

$$\begin{aligned}
\frac{1}{2}\phi(r_i) + \sum_{j=1}^N \phi(r_j) \oint_{\Gamma_j} \phi(r') \frac{\partial G(r', r_i)}{\partial n(r')} d\Gamma(r') \\
+ \sum_{j=N_{in}+1}^{N_{in}+N_\alpha} \phi(r_j) h(r_j) \oint_{\Gamma_j} \partial G(r', r_i) d\Gamma(r') \\
= - \sum_{j=1}^{N_{in}} I(r_j) \oint_{\Gamma_j} \partial G(r', r_i) d\Gamma(r') + P_S G(r_s, r_i)
\end{aligned} \tag{2.14}$$

Where  $i = 1, 2, \dots, N$  corresponds to different collocation points. For each collocation point there is one  $\phi(r_i)$  equation which depends on integration over all surface elements  $\Gamma_j$ . All equations are put in a matrix and the matrix is solved to give the boundary potential values  $\phi(r_i)$ . Once the intensity potential equation is solved for the boundaries, the results can be applied to calculate  $\phi(r)$  values for all the field points:

$$\begin{aligned}
\phi(r) = - \sum_{j=1}^N \phi(r_j) \oint_{\Gamma_j} \frac{\partial G(r', r_i)}{\partial n(r')} d\Gamma(r') \\
- \sum_{j=N_{in}+1}^{N_{in}+N_\alpha} \phi(r_j) h(r_j) \oint_{\Gamma_j} G(r', r_i) d\Gamma(r') \\
- \sum_{j=1}^{N_{in}} I_{in}(r_j) \oint_{\Gamma_j} \partial G(r', r_i) d\Gamma(r') + P_S G(r_s, r_i)
\end{aligned} \tag{2.15}$$

### 2.3. 3D models

The 3D CAD models which are used in BEMIPA code for simulating the sound field due to the engine noise were created using NX-3 GME version at Saab, Trollhättan. The meshed models which are used in this project are taken from Onur Atak's thesis [7]. In [7] these models are introduced as detailed and simplified models.

When meshing the geometry for BEM calculations one important thing to consider is the element size. In BEM, size of elements should be set in a way that can sufficiently present the spatial variations of the field. The sufficiency of the mesh elements depends on the requirements and formulae in the method. Atak used Helmholtz equation to model the sound propagation properties which is based on wave equation. Therefore his model was dependent on the wavelength and to model the sound field at higher frequencies with smaller wavelengths he had to choose smaller element sizes. Although the element sizes in his work are set to be suitable for

frequencies up to 1 kHz and plates with minimum thickness of 5mm, they are still appropriate for high frequencies in BEMIPA calculations. The reason is that in BEMIPA the sound field is modelled using intensity potential which varies slowly in space and is only dependent on the geometry of the system not the frequency. As a result, as long as the elements can cover the required geometrical details of the system they are fine for the BEMIPA model.

In Atak's work different configurations of the model are tested and the model is modified couple of times to obtain the closest simplified geometry to the real engine bay. For this reason the radiator and cooler fan are removed from the CAD model, because in reality the radiator is acoustically transparent to perpendicular incoming sound waves. Another modification that was tested by Atak includes an artificial back part in front of the firewall which simulates the cables, pipes and containers that are densely packed in this region. The back part is modelled with a box. Dimensions of the box are  $750 \times 480 \times 100$  mm and there are a number of holes with various sizes on it.

Three configurations of engine bay model developed in Atak's work are studied in this project. These configurations are known as Detailed model without cooler and back part, Simplified model without cooler and back part and Simplified model without cooler and including the back part. Figure 2.1 and Figure 2.2 show the CAD models of the simplified and detailed geometries [7].

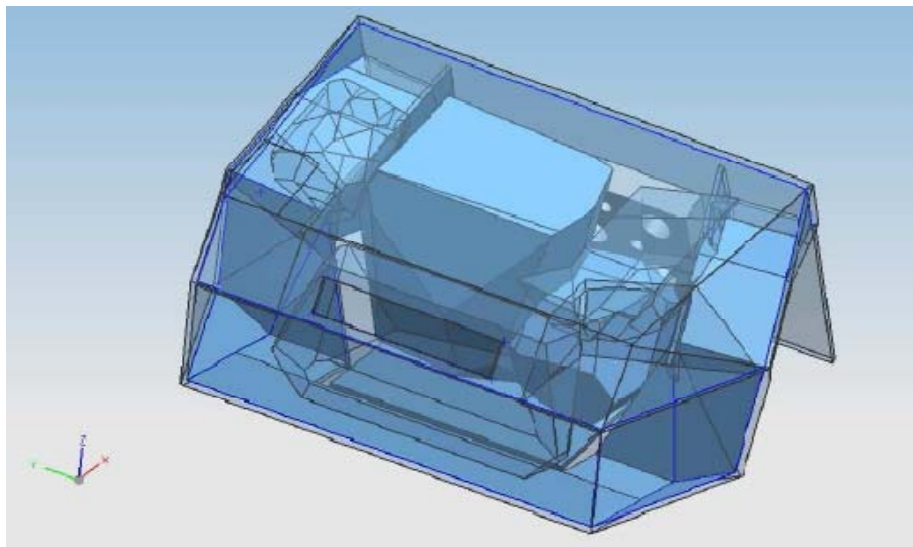


Figure 2.1: Simplified model without the cooler and including the back part (the simplified model without the back part is the same as this model but only the perforated back part is not included in it)

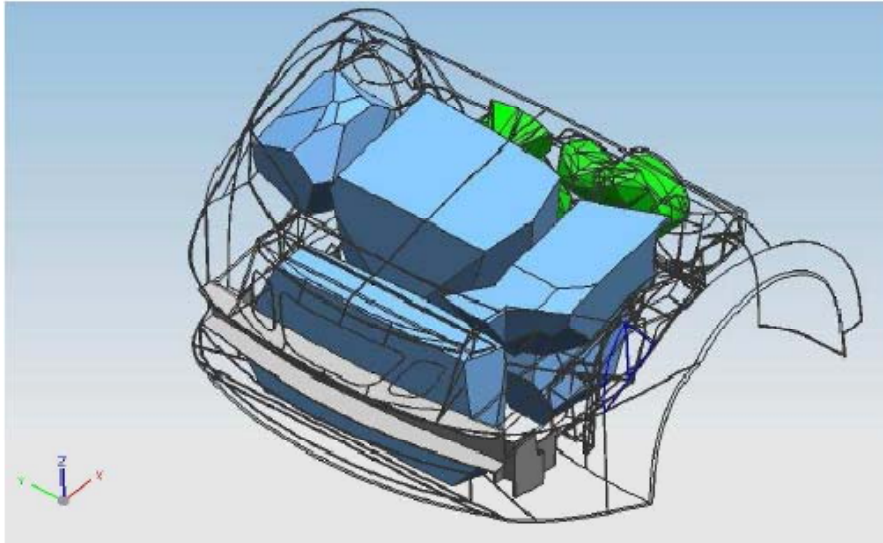


Figure 2.2: Detailed model without the cooler and back part

One can notice the differences between simplified and detailed models from the figures above and it is also obvious that the detailed model is not exactly like the real engine bay. Atak explained in his thesis that meshing a complex geometry like an engine bay required large number of mesh elements which could have led to very long calculation times and needed huge amount of computer RAM, so the actual model of engine bay created by Saab has been simplified in Atak's work and current detailed model is in fact a simplified version of the real engine bay lacking many pipes, cables and accessory parts.

## 2.4. Scattering objects

Inside an engine bay there are many accessory parts such as pipes and cables which due to their shapes and sizes are able to scatter the sound waves. At high frequencies where the dimensions of these accessory parts are in the order of wavelengths, the scattering effect of these objects becomes more highlighted.

In [8], Lindberg and Andersson investigate the sound scattering effects of accessory parts in an engine bay by studying sound radiation from the engine bay of a passenger car, a simplified hardware model of engine bay and a numerical model based on FEM. In the hardware and numerical models different configurations of the interior objects are tested and variations of the radiated sound field due to each configuration is studied.

The investigations show that the total radiated sound power is very dependent on the density of the scattering objects and the frequency [8]. The results state that the increase of scattering objects together with the increase of frequency, generally reduce the radiated power levels. As the paper denotes, the accessory parts reflect and scatter the sound waves and increase the number of reflections towards the absorbing surfaces, which gives an increase in the amount of absorbed power. In other words, the high density of accessory parts in the engine bay besides the high

frequency range of sound waves would add extra absorption to the field apart from the actual absorption properties of different surfaces.

On the other hand, including the details of geometry like pipes, wires and other small objects inside an engine bay could be a quite time consuming step when setting up the geometry, meshing the model and assigning boundary conditions. It could also make the calculation time unrealistically long. Therefore, based on the explanation presented above, in the geometry models, it would be reasonable to replace the small problematic accessory parts with an extent of additional absorption on the proper surfaces of the engine bay.

## 2.5. Model of absorbers

When simulating the sound field at high frequencies nothing is more important than assigning proper absorption properties to proper surfaces. Absorbing surfaces of the engine bay models are divided into two categories regarding their absorption properties, main absorbers and equivalent scattering absorbers.

Main absorbers which in reality are specially designed surfaces to absorb the noise of the engine bay consist of under-tray, hood and firewall. These parts are selected based on their real absorption properties in the three Saab vehicles. The surface of main absorbers in the real engine bays is either subjected to specific sound treatments like installing extra absorbers or has noticeable irregularities which can scatter the sound waves and attenuate their energy.

All the other surfaces in the engine bay models -rather than the main absorbers- are introduced as equivalent scattering absorbers. They have a lower absorption coefficient compared to the main absorbers, but they are still very important in absorbing the sound and reducing the noise levels in the engine bay. It was explained earlier that the accessory parts are better be excluded from the geometry models due to the complexities they could cause in the simulations. However, regarding the fact that these objects occupy a large ratio of space in the engine bay and usually have small dimensions in the order of wavelengths at high frequencies, they can play a major role in scattering the sound waves and increasing the sound absorption in the engine bay. Consequently, their sound absorptive influence should definitely be included in the modellings in some way.

Atak showed in his thesis that it is possible to neglect the scattering objects in the geometry models and then compensate their sound absorptive effect by assigning an equivalent absorption to all the surfaces (except the main absorbers) inside the engine bay model [7]. Since the absorption coefficient values that he used for these surfaces showed quite good results in his simulations up to 1 kHz, the same input data were applied for modelling equivalent scattering absorbers in current thesis.

As the first step of modelling the absorption characteristics of both surface categories, acoustic impedance of the surfaces is calculated. BEMIPA allows directly

assigning an angle-dependent absorption curve to the surfaces, but to keep the consistency with Atak's work and use his input data, also to obtain the dependence of the surface absorption to the angle of incidence, the acoustic impedance is calculated in this step.

To calculate surface impedance, Delany-Bazley model for characteristic impedance of porous absorbers is applied:

$$Z_c = \rho_0 c [1 + 0.0571 \left(\frac{\rho_0 c}{\sigma}\right)^{-0.754} - j0.087 \left(\frac{\rho_0 c}{\sigma}\right)^{-0.732}] \quad (2.16)$$

where  $\rho_0$  and  $c$  are density of air and speed of sound in air respectively and  $\sigma$  is flow resistivity of the surface.

Using the resulting  $Z_c$  values, the impedance of a surface with a specific thickness can be calculated from equation (2.17):

$$Z_{abs} = Z_c \coth(kL) \quad (2.17)$$

where  $k$  is the wavenumber defined as::

$$k = \frac{\omega}{c} [1 + 0.0978 \left(\frac{\rho_0 c}{\sigma}\right)^{-0.7} - j0.189 \left(\frac{\rho_0 c}{\sigma}\right)^{-0.595}] \quad (2.18)$$

Depending on which category the surface belongs to, the input values to  $Z_c$  equation differ and consequently the absorption values differ. The values which are used as the input to Delany-Bazley formula for both of the absorber categories are taken from Atak's thesis data.

To calculate the absorption coefficient of the surfaces, two approaches can be applied. The first approach is to consider the condition that incoming waves have a normal incidence on the surface. For this case the reflection coefficient would be:

$$r_{normal} = \frac{Z - \rho c}{Z + \rho c} \quad (2.19)$$

The absorption coefficient could be calculated using equation (2.20).

$$\alpha = 1 - |r|^2 = \frac{W_{loss}}{W_{in}} \quad (2.20)$$

Another approach is to assume a diffuse incidence condition meaning that the probability of incidence is the same for all directions. Möbius used a formula to calculate the diffuse absorption coefficient [9]. In reality the high-frequency sound waves have a condition between these two approaches meaning that they hit the surface from different angles but assuming a perfect diffuse field is also an over-estimation. Being in the vicinity of one reflecting, absorbing or scattering surface adds directivity to the sound radiating from a source which violates the assumption of a perfect diffuse field. However using diffuse incidence assumption is not quite unrealistic since in the real acoustic field of a high-frequency noise when there are many scattering objects in the volume, the sound waves may move in every direction

and hit the surfaces in the domain with any angle, so using diffuse incidence condition can be a more reasonable approximation rather than normal incidence assumption. For this assumption equation (2.19) can be rewritten as:

$$r = \frac{Z \cos \varphi - \rho c}{Z \cos \varphi + \rho c} \quad (2.21)$$

where  $\varphi$  is the angle between the incident wave and the normal to the surface at the point of incidence,  $Z$  is the surface impedance,  $\rho$  is the density of the medium and  $c$  is the speed of sound in the medium.

Absorption coefficient should be calculated by integrating over all angles around the surface. By taking an infinitesimal area on the surface of a sphere defined as:

$$dS = R^2 \sin(\theta) d\theta d\varphi \quad (2.22)$$

using equation (2.20) and integrating over a half sphere surface, the following formula for diffuse incidence absorption coefficient is obtained [9]:

$$\alpha_{diffuse} = \int_0^{\pi/2} 2 \alpha \cdot \cos \varphi \cdot \sin \varphi \cdot d\varphi \quad (2.23)$$

However, as expressed in section 2.2, to define the absorption properties of the surfaces in this project  $\langle \varepsilon(r, \theta) \rangle_\theta$  which is a function of absorption coefficient of the surface is applied instead of  $\alpha_{diffuse}$ . Therefore, to define angle dependence in the incident waves, first equations (2.11) and (2.21) are used to include the angle dependence in the formulations, then it is assumed that the incident power is uniformly distributed over the surface which leads to equation (2.12) for  $\langle \varepsilon(r, \theta) \rangle_\theta$  that expresses the absorption properties of the surface for the diffuse incidence.

Section 5.3 covers more discussions about differences between normal incidence and diffuse incidence approaches.

### 3. Measurements

The measurement data which are used to compare with the simulation results are taken from the engine bays of Saab 9-3, Cadillac BLS Station Wagon and Cadillac BLS Sedan. All three engine bays are constructed based on General Motors Epsilon architecture and except for some small details, they are similar. The only engine which has a different acoustic treatment compared to the others is Cadillac BLS Sedan but the treatment in this engine is mainly focused on reduction of sound transmission to the passengers' cabin and there are also some extra absorption in front of the dash and edges of the hood.

Measurements were performed using 14 point sources at the height of 0.75 m as shown in Figure 3.1. More details about the measurements procedure can be found in [6].

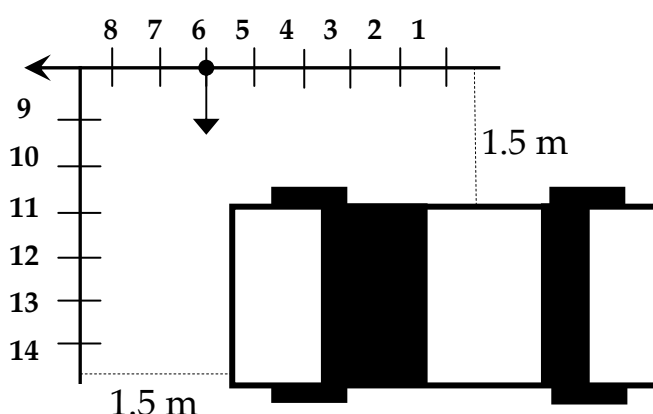


Figure 3.1: Source positions in engine bay measurements. The distance between each position is 0.5 m.

There are 60 measurement points on the engine bay for the first measurement and 20 for second and third. Every set of measurement contains the FRFs between the microphones connected to every source and the microphones at different positions inside the engine bay. Measurement outputs were converted to sound pressure normalized to volume velocity of the source after calibration,  $p/U_\omega$ .

For measurements, instead of installing many point sources with the same sound power on the engine bay, the sources were placed outside of the engine bay as shown in Figure 3.1 and microphones were placed at different positions inside of it. Although in reality the noise radiates from the inside of the engine bay and is received at the outside, but since frequency response functions (FRFs) between these points are of our interest, based on the reciprocity of FRFs this contradiction will not



be a problem. To keep the consistency with Atak's thesis, from now on the sources outside of the engine bay will be called receivers and microphone positions inside the engine bay will be named as sources.

## 4. Calculations

The outputs of BEMIPA are transfer functions of intensity vectors over sound power emitted from the source,  $I(r)/P_s$  while the measurement outputs are sound pressure normalized to volume velocity of the source after calibration,  $p/U_\omega$ . To investigate the correctness of the model a comparison should be done between the calculations and measurements. Therefore the FRFs should be converted to a comparable quantity. Volume velocity is converted to input power using

$$P_s = \left(1 + \frac{\sin(2kd)}{2kd}\right) \frac{\rho_0 \omega^2}{8\pi c_0} |U|^2 \quad (4.1)$$

Where  $k = \omega/c_0$  is the wavenumber,  $c_0$  is speed of sound in the medium,  $d$  is the distance to the closest surface,  $\rho_0$  is the density of medium,  $\omega$  is the angular frequency and  $U$  is the volume velocity of the source. There are a number of assumptions behind equation (4.1) expressing that only the reflection from the closest surface contributes to the impedance at the source position and this surface is assumed to be acoustically rigid, perfectly flat and of infinite extension. The relation between sound pressure and sound intensity in the field points is formed based on the far field impedance approximation.

$$\|I(r)\| = \frac{1}{2} \frac{|p(r)|^2}{\rho_0 c_0} \quad (4.2)$$

Where  $\|I(r)\|$  represents the L2-norm of the intensity vector. The final relation which is used to convert measured  $p/U_\omega$  values to  $I(r)/P_s$  is presented below [2].

$$\frac{\|I(r)\|}{P_s} = \frac{4\pi}{\left(1 + \frac{\sin(2kd)}{2kd}\right) \rho_0^2 \omega^2} \left| \frac{p(r)}{U} \right|^2 \quad (4.3)$$

### 4.1. Selected source positions for calculations

To make the calculation process shorter and save more time for deeper investigation on different aspects of the method, we have not modelled radiation from all of the measurement sources. Instead, a few number of sources at four different regions of the engine bay are selected for evaluation of the BEMIPA code as well as studying the radiation properties of the engine bay. When investigating radiation from single sources, one source per region is picked for calculations and when total radiated

power from several sources is of interest more than 5 source positions per region are used for simulation.

Selecting sources from different regions of the engine bay gives more informative and assuring calculation results about the correctness of the model. Each region is labelled based on the main source in that region which is used in single source calculations. Main sources which are called after their microphone labels are A06, B2, B24 and B32, see Figure 4.1 to Figure 4.4. These sources have also been used in Atak's thesis for investigation on low frequency range (up to 1 kHz).

Source **A06** is located beneath the engine in the front. This position is 18 cm above the undertray. See Figure 4.1.

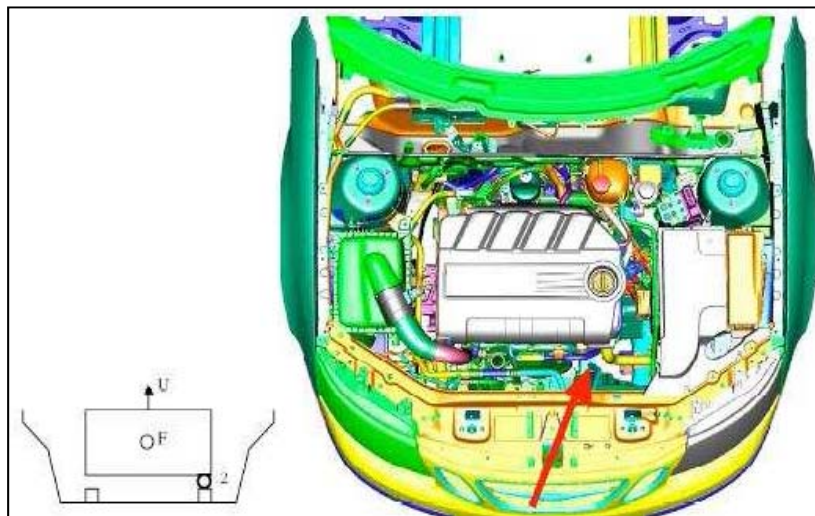


Figure 4.1: Source position A06 (labeled as number 2 in the sketch)

Source **B2** is located on the left side of the engine and is close to the hood absorber. See Figure 4.2

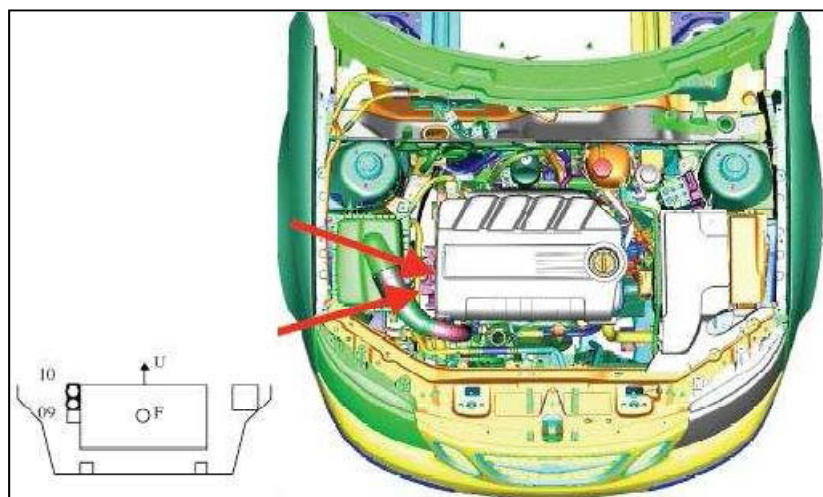


Figure 4.2: Source position B2 (labeled as number 10 in the sketch)

Source **B24** is at the back of the engine bay and is close to the dash part. This source is located almost in the middle of engine's height. See Figure 4.3.

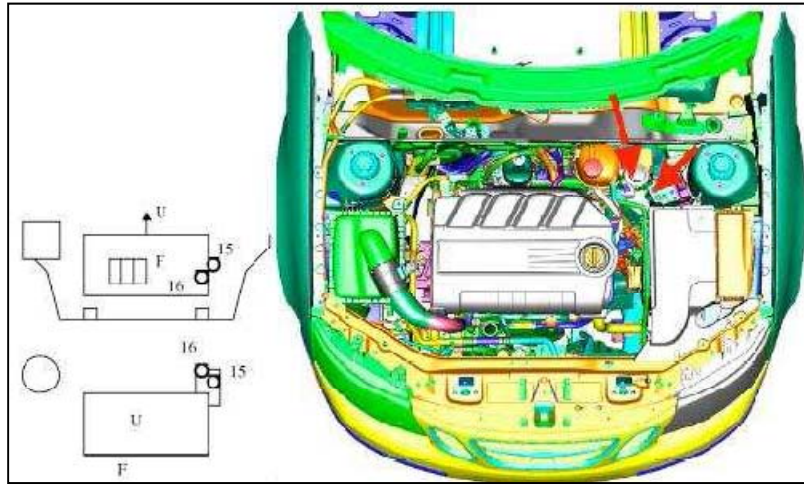


Figure 4.3: Source position B24 (labeled as number 16 in the sketches)

Source **B32** is on the left side of the battery box and is close to the front of engine bay. See Figure 4.4.

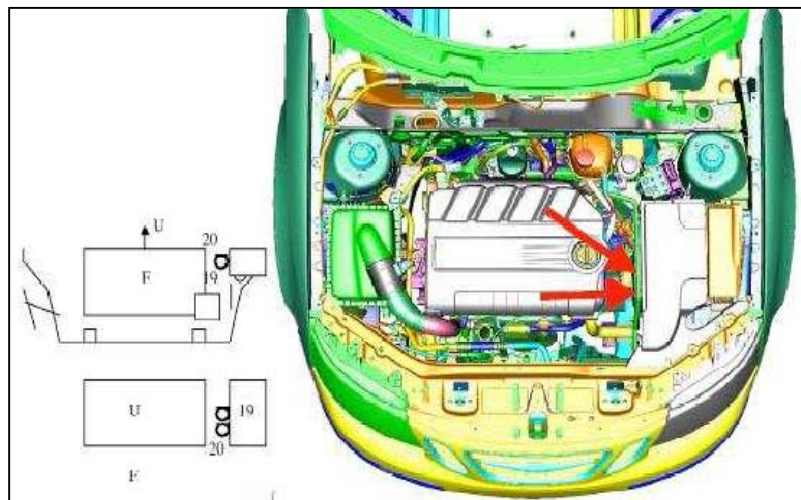


Figure 4.4: Source position B32 (labeled as number 20 in the sketches)

## 5. Results: Understanding the acoustic behaviour of BEMIPA

The behaviour of the BEMIPA method under different conditions is studied in this section. The subjects of investigation are sensitivity of the method to geometrical variations and the influence of the absorption properties on the simulation results.

Studying on the geometrical variations effect starts with running calculations for the two simplified models. Starting with simple geometries can both save a lot of calculation time and give a view of how the method responds to small geometrical differences. Once the behaviour of the method for simplified models and its deviation from the real engines measurement outputs is realized, the investigations are expanded to take the detailed model effect into consideration.

Different aspects of absorbing surfaces are examined to obtain a clear view of the influence of absorption properties of the field on the simulation results. These aspects include the absorption coefficient curves of the surfaces, the approach which is applied to calculate these absorption coefficients and the position of absorbers in the engine bay. An investigation on the effect of the distance between source and absorber on the absorption of radiated sound waves is presented in Appendix B.

During the investigations, the simulation results are always compared with the measurement curves. The metric which is used to compare them is averaged level of energy transfer functions [3].

In advance to presenting the result curves it should be mentioned that some primary tests showed that the average intensity curves over all receivers at high frequencies are quite smooth (with variation less than 6dB over a quite broad frequency band), so it is not required to use a high frequency resolution in the calculations. Therefore, to reduce the calculation time, only 7 of the third-octave centre frequencies between 1 to 10 kHz were picked for sound intensity calculations. Later comparisons will show that this simplification has not affected the quality of presented results.

It is also important to point out that all along the results sections, the calculation and measurement curves plotted for the engine bays represent the energy transfer functions averaged over 14 receiver positions as are shown in Figure 3.1. In addition, due to the similarity of the results for different source positions in many of the investigations, in this section whenever there is the same tendency among the results only the graphs corresponding to the source B24 is presented and the rest of the curves are given in Appendix A.

## 5.1. Investigation on different geometry models

### 5.1.1. Simplified geometries

Figure A.1 illustrates the calculated curve by BEMIPA for the most simplified engine bay model which is called “simplified model without the back part”. In this figure the calculated levels of acoustic energy radiated from a single source are compared with the corresponding measurement data taken from the real engine bays.

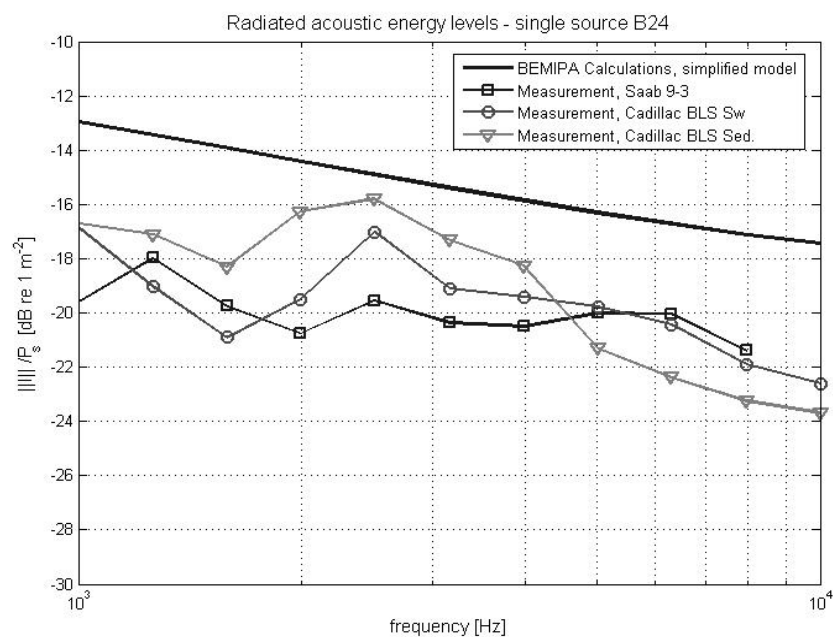


Figure 5.1: Single source B24 - Calculated values are based on *simplified model without the back part* and measurements are performed on three engine bays with similar construction but difference in details.

Comparing the simulation and measurement curves shows a similar behaviour between the calculated and measured curves. In both cases the radiated acoustic energy levels decrease gradually by increasing the frequency and the curves have smooth variation in a large frequency range from 1 to 10 kHz. It is also noteworthy that the difference between simulation results and the measurement data does not exceed 7dB. These results show that the model is well capable of predicting the general behaviour of the radiated sound power curves. On the other hand, the calculated curves do not represent the peaks and dips as is visible in the measurement curves. This is quite reasonable, because the calculations are based on the heat transfer analogy and energy transfer from higher density to lower density regions. In this analogy the interference of the sound waves and resonance effects which can cause vortices and irregularities in the field are not included. However, our aim which is predicting the general behaviour of radiated sound field from many similar individuals with differences only in details is expected to be fulfilled with

current method. It is also expected that the difference between calculations and measurements becomes smaller by applying a more realistic geometry model.

In the next step, radiation from another simplified model which includes an extra object called “back part” is investigated. It was mentioned before that the back part is placed in front of the firewall in the model to simulate the accessory parts and containers which are densely packed in this area of the real engine bays. Regarding the dimensions of the back part,  $750 \times 480 \times 100$  mm, it is expected that this new object can partly block the power flow to the openings at the back, leading to reduced noise levels at the receivers.

Figure 5.2 shows the effect of including the back part in the calculations.

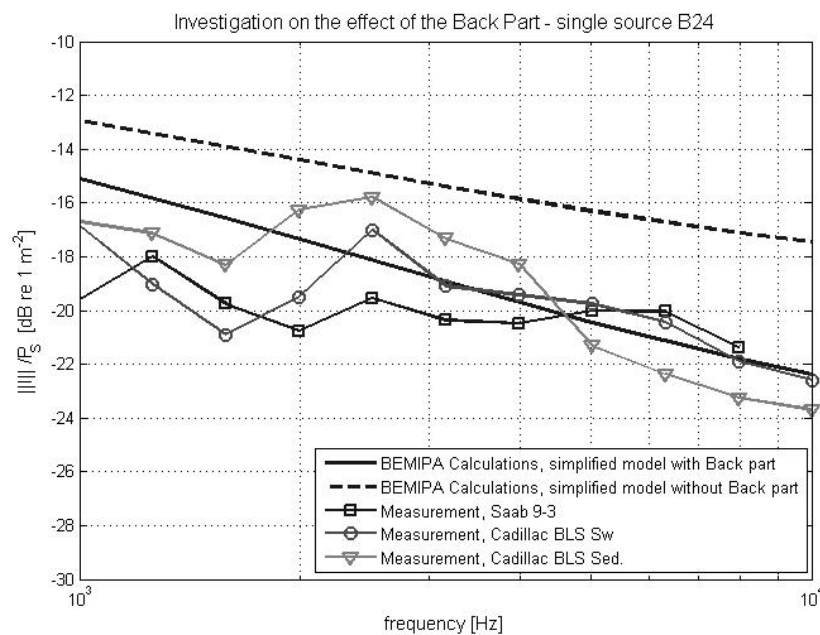


Figure 5.2: Single source B24 - Calculated values are based on the two *simplified models with and without the back part* and measurements are performed on three engine bays with similar construction but difference in details.

Looking at the difference between calculated curves for the two simplified configurations of engine bay and comparing Figure 5.2 with the similar figures for other source positions (appendix A.2), one could conclude that the effect of including an extra object varies for different source positions. Presence of the back part causes a noticeable decrease in the radiated sound power from B24, but this object cannot efficiently block the power flow from other sources. Effect of the back part on the radiation from sources A06 and B2 is so small that the calculated curves for the two models have almost the same values and shapes. Also, for source B32 the difference between these curves is less than 0.4 dB. These results can be explained by the position of each source relative to the added object.

Source B24 is very close to the back part compared to other sources and it is more likely to be affected by this object. In the previous simplified model the area in front

of the firewall was empty and the sound waves emitting from B24 could escape from the opening in the back, but when the back part is included a large ratio of the waves would be blocked. Based on this result, one could suggest that when geometrically and technically possible, installing more blocking objects in front of the openings can reduce the radiated sound from noise sources at different regions of the engine bay. Aside from source B24, other sources are either very far from the back part (e.g. source A06 and B32) or very close to a strong main absorber (source B2 is very close to the hood absorber), so the presence of the back part does not have a distinctive effect on the sound radiation from them.

### 5.1.2. Detailed geometry

Detailed geometry is the most similar model to the real engine bay. Although it does not include many details (e.g. pipes and cables), it is still closer to the real engine bays geometry compared to the simplified models.

The detailed model does not include the back part which acts as some accessory parts in the engine bay, but instead it contains some engine walls and beams which exist in the real engine bays and are not included in the simplified models. Like in the previous geometries, the lack of scattering objects in the detailed model is compensated by assigning equivalent scattering absorption to all the surfaces other than the main absorbers.

Figure 5.3 illustrates calculated energy transfer function curve based on the detailed model and compares it with corresponding curves based on measurements and the simplified model calculations (simplified model without the back part).

For almost all of the source positions (except B2), when using detailed model instead of simplified model, the simulation curves become closer to the measurement results. It shows how just by using a slightly more realistic geometry model in the simulations, the BEMIPA method can provide a quite better prediction of the sound field.

Investigation on different source positions shows that except for source B2, the detailed model curve corresponding to all the other three source positions has lower levels compared to the simplified model. The behaviour of radiation from source B2 is completely different from other source positions. The power level due to the detailed geometry for B2 is higher than the simplified model curves. Also, detailed model shows larger deviation from the measurements compared to the simplified model; this behaviour is presented in Figure 5.4.



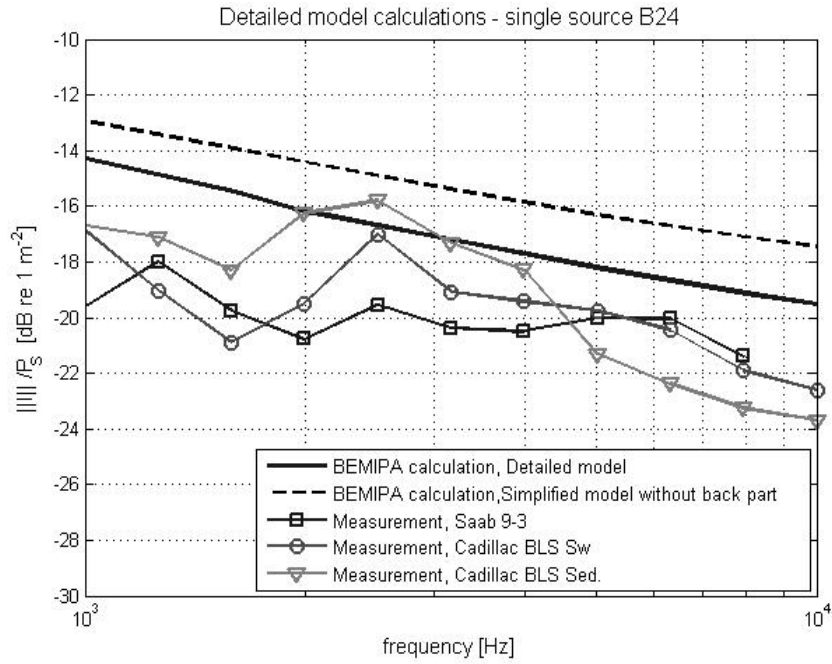


Figure 5.3: Single source B24 - Calculated values are based on *detailed model and simplified model without the back part* and measurements are performed on three engine bays with similar construction but difference in details.

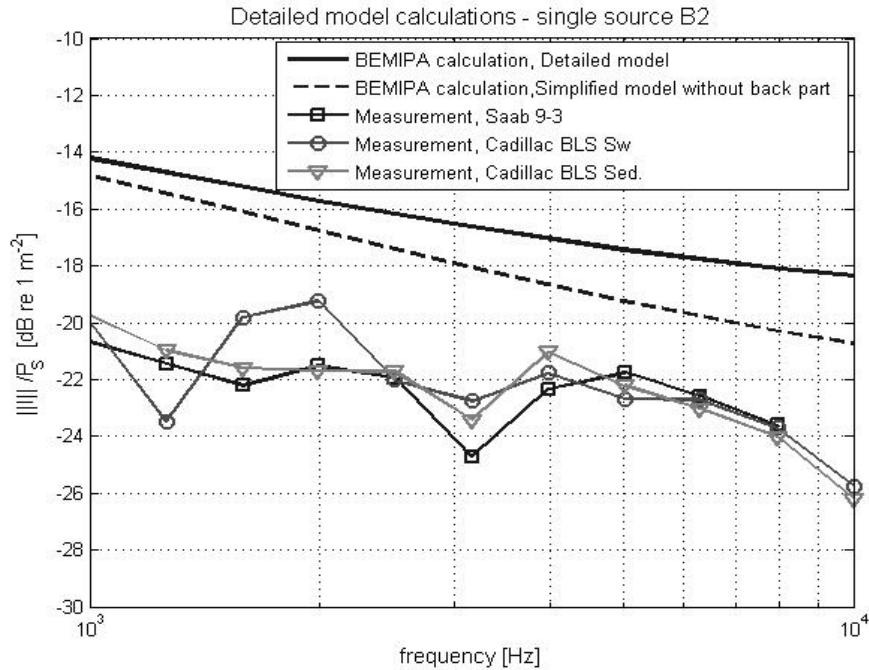


Figure 5.4: Single source B2 - Calculated values are based on *detailed model and simplified model without the back part* and measurements are performed on three engine bays with similar construction but difference in details.

### 5.1.3. Comparing the results of different geometry models

Comparing different models for each source position shows that for single sources A06 and B32 using the detailed model gives lower radiation levels compared to the simplified models. This reduction is quite large for radiation from single source A06 (about 4dB on average) which shows the high sensitivity of the radiation from the source in this position to the geometrical changes of the model.

The low predicted levels for source A06 in the detailed model can be explained by the position of this source relative to one of the plates which is added to detailed geometry and is not included in the simplified models. A06 is positioned behind this plate, so the direct path which exists between this source and the opening in front of the engine bay in the simplified models is blocked by this additional part. This prevents many of the sound waves from radiating directly to the exterior and instead reflects them toward different surfaces of the engine bay including the absorbers. This leads to absorption of more sound waves and consequently reduction of the radiated power level in the detailed model.

Calculated energy transfer function curve based on the detailed model for source B2 is even 2dB higher on average compared to the simplified models. It was explained before that since B2 is positioned on top of the engine bay very close to the hood absorber, sound radiation from this source is dominated by the high absorption of the hood and it can be the reason for matching of the simplified model curves. However in the detailed model there are some extra objects included which can possibly misdirect the sound waves and prevent them from reaching to the main absorbers in the lower regions of the engine bay but instead, reflect and scatter them towards the openings of the engine bay and cause higher radiated levels.

For source B24 although the sound power levels calculated based on detailed model are lower than the results of simplified model without the back part, but they are higher than calculated values for simplified model including the back part. This can be explained regarding the effect of the back part as both a sound blocking and sound absorbing object. Source B24 is very close to the back part and highly affected by this object. In the detailed model the back part is not included, so actually the back of the model is open and it is a very good way for sound waves to escape. This is why the radiation values in the detailed model and simplified model without the back part are higher than the simplified model including the back part. However detailed model still presents lower radiated power than simplified model without the back part due to the absorbing effect of additional objects which are included in the detailed geometry.

The sound field due to source B32 is mainly affected by the total absorption of the system, so when the detailed model is used and more surfaces with an extent of absorption are added to the system the radiated power decreases correspondingly.

## 5.2. Modelling and measurement differences

Investigating the difference between measurement results and calculated curves for different geometry models showed that in the majority of the cases there is few decibels difference between measurements and calculations (less than 6dB). This shows that BEMIPA method is a rather strong tool for prediction of the averaged total sound radiation from sources in a partial enclosure. However one should consider that there still exist some decibels difference between total radiated energy obtained from measurements and the calculations. This difference can be explained by a number of reasons as written below:

- It is mentioned in [2] that IPA can predict the global radiated power, but a fundamental limitation of this method is that the radiation to specific regions or specific field points may not be well captured by the method. Calculating the global radiated power requires making average over many receivers which can represent a large part of the space, while in this project to keep consistency with the measurement conditions we are limited to take the averages over only 14 receivers all at the same height in a limited region.
- So far only the total averaged fields obtained from single sources are calculated. Some of these single sources are very close to the walls or plates in the engine bay, so the radiated sound waves from the source can hit these surfaces with few number of angles. This form of incidence can be defined as a sort of directivity in the radiated power from the source to the surface which is a violation of the assumption that is used in IPA for derivation of the boundary condition for an absorber. The assumption is that the sound waves hit the surface from several directions and different angles. Therefore it is expected that IPA perform better for a sound field which is created by several radiating sources.
- There are uncertainties in both engine bay geometry and the coordinates of the source positions in the models which can cause some errors in calculations.
- The uncertainties existing in the applied boundary conditions can be another source of errors. These boundary conditions include absorption curves, Delany-Bazley absorber model, locally reacting surface assumption, which surfaces should have what boundary conditions, etc.
- Pipes, wires, accessory parts and other engine bay details are not included in the geometry and their effect is only approximated by the "equivalent scattering absorption". Since the approximation cannot be perfect, some differences are expected to appear between measurements and calculations.
- The measurement data are taken from only three engine bays and although they have similar designs, there is still couple of decibels difference between their measured power level curves. Therefore it cannot be expected that the simulation be able to predict the radiated power for all of these individuals perfectly.

- As is shown in master's thesis by Schönfeld [10] or in Corakci and Tober's work [11], in energy-based sound field prediction methods like SEA or IPA despite the effort which is made to bring simulation results close to the measured data, there is always a few decibels difference between these values.

### 5.3. Absorption effect

This part mainly focuses on the importance of the absorption properties of the surfaces in the models.

In section 2.5 it was explained that two approaches can be used to calculate absorption coefficients of different surfaces in the engine bay, normal incidence and diffuse incidence. In this project, all of the  $\langle \varepsilon(r, \theta) \rangle_\theta$  values have been calculated based on the uniformly distribution of the sound waves over the surface of an absorber. Although it might be considered as an over-estimation of diffusivity of the sound field in the engine bay, actually in reality there is a high possibility that the sound waves hit the surface at many different angles. Especially when high frequencies are of interest and there are many objects of different sizes around the source, the chance of getting close to a diffuse field becomes higher. In this condition the probability of incidence is the same for all directions and the absorption coefficient should be calculated by integrating over all the angles around the surface shaping a half-sphere.

Figure 5.5 and Figure 5.6 present the comparison between absorption coefficient curves calculated based on the normal and diffuse incidence of the sound waves. The graphs also show absorption coefficient curves of an ideal surface with  $Z = \rho c$  for these approaches.

The normal and diffuse incidence absorption coefficient curves for main absorbers are convergent and they have almost the same values at high frequencies above 5 kHz. Both of these curves are very close to the absorption coefficient of an ideal surface which means that in this range, no matter what approach is used, the high absorption of the surface determines the absorption coefficient values and makes the surface act closely to an ideal surface.

Unlike the main absorbers, absorption coefficient curve for the rest of surfaces in the engine bay is very dependent on the approach which is taken to calculate  $\alpha$ . As Figure 5.6 illustrates, there is a significant difference between the normal and diffuse incidence absorption curves for the rest of surfaces which are assigned with equivalent scattering absorption properties. Regarding this dependence of  $\alpha$  on calculation approaches and on the other hand due to the fact that the scattering objects fill a large ratio of space inside the engine bay and play an important role in formation of the sound field, one could conclude that choosing a proper approach for

calculation of absorption coefficients for the rest of surfaces is highly influencing in the modelling.

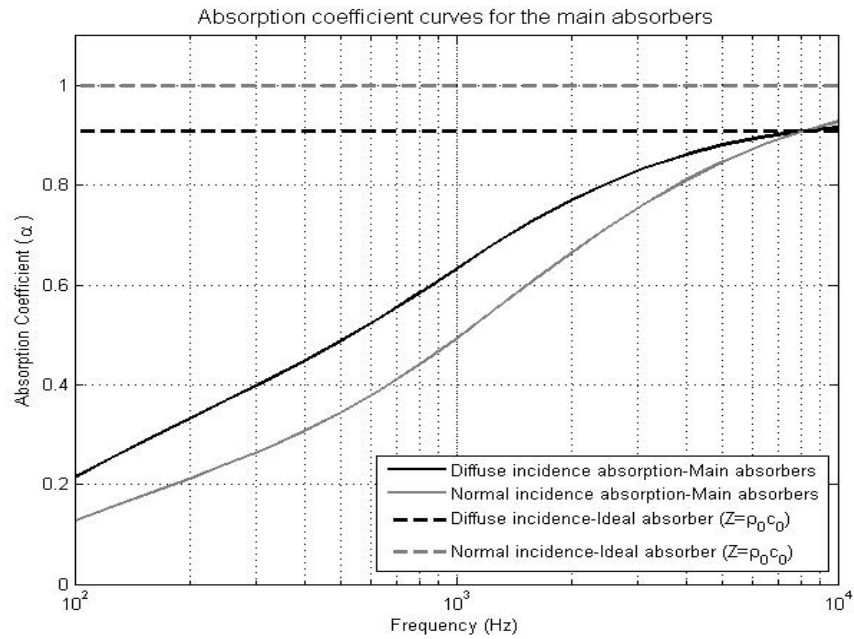


Figure 5.5: Normal and diffuse incidence absorption coefficients for the main absorbers and an ideal absorber

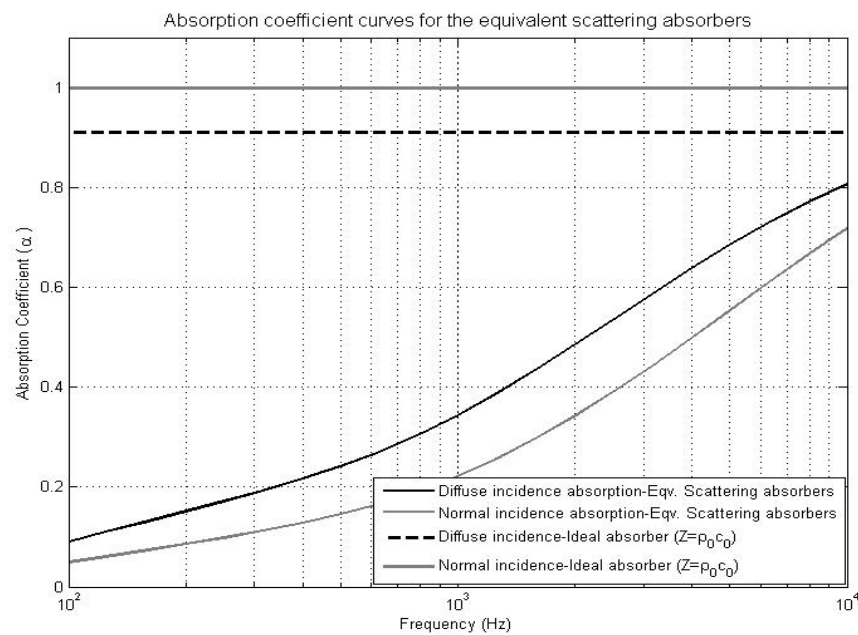


Figure 5.6: Normal and diffuse incidence absorption coefficients for the rest of absorbers and an ideal absorber

Another investigation about the absorption effect was to study whether increasing the absorption of the surfaces in a way that they act as ideal surfaces can provide a lower radiation or not and to what extent this modification can help to make a quieter engine bay. Here, whenever used, ideal absorber or ideal surface mean surfaces with  $Z = \rho c$ .

First, all of the surfaces were assigned with  $Z = \rho c$  which is a property of ideal surfaces. Then the resulting radiation curves due to this change were compared with the common absorbers' curves. In the next step, only the main absorbers were assigned with ideal  $Z$  value. In reality, these surfaces are mainly responsible for absorbing the radiated noise from the engine bay due to the noise reduction treatments which is applied on them, so it would be interesting to see how effective they can be as ideal absorbers.

### 5.3.1. Effect of ideal absorber on all surfaces

An extreme case which all the surfaces inside the engine bay are covered with ideal absorbers is studied here. The purpose is to see what would be the lowest possible sound levels that one could achieve only by increasing the absorption levels to the maximum levels. The high absorptive model is then compared with the normal model with common absorbers. Since the difference between two conditions for one geometry is of our interest, it would be enough to do this comparison only for one of the geometry models. To save more time, only the simplified geometry including the back part is picked for the test. In this section, whenever used, by "model with common absorbers" we mean the model in which the main absorption coefficient curve is applied on the main absorbers and equivalent scattering absorption curve to the rest of surfaces. Figure 5.7 shows the results of our investigation for source B24. The graphs corresponding to other source positions are presented in Appendix A. Like in the previous graphs, measured and calculated curves in this figure show energy transfer functions averaged over 14 receiver points.

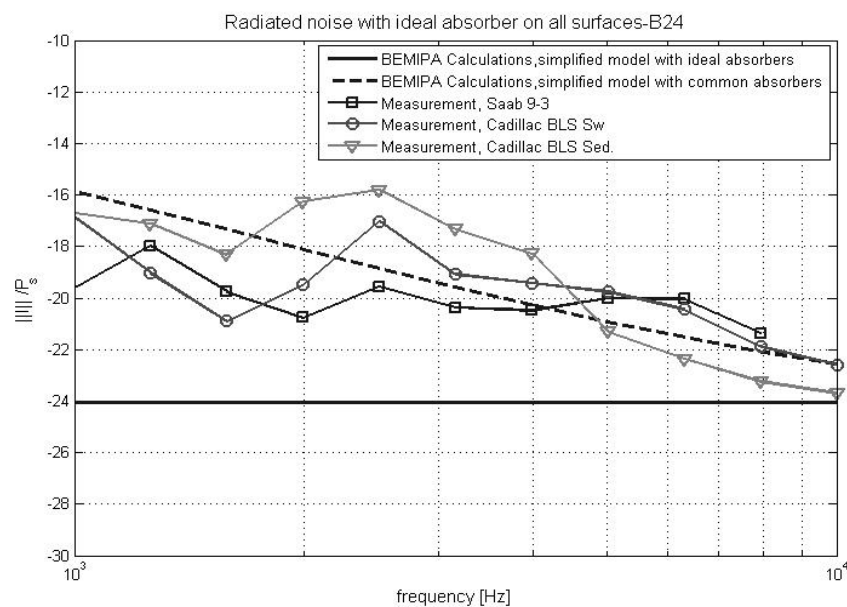


Figure 5.7: Single source B24 - Calculated values are based on simplified model including the back part for two situations: 1-The surfaces are assigned with Main and Equivalent scattering absorption properties 2- All surfaces are assigned with ideal absorption.

The solid black curve in Figure 5.7 shows the case that all surfaces are assigned with  $Z = \rho c$  at all frequencies. For all of the source positions, using this ideal absorption gives a large reduction at lower frequencies (maximum 8dB at 1kHz), but at higher frequencies the difference between the curves of the two absorption models decreases to reach about less than 2dB at 10kHz. This can be explained by the fact that at higher frequencies, the absorption coefficient of the porous absorbers which are used as common absorbers in the simulations increases and their behaviour becomes very close to ideal absorbers. Another noteworthy point in this test is that the calculated curves based on the ideal absorbers are not much different from measurement curves. The difference between these curves is maximum 5dB and even at very high frequencies the estimated radiated power based on the ideal absorber is sometimes higher than the measurement results. There can be two reasons for this result; one is due to the weakness of the simplified model in presenting the real properties of the engine bay and the other is due to the insufficiency of absorbers in absorbing the sound.

Simplified model may have weakness in showing the exact behaviour of the real engine bay and consequently it might not be able to present the real effect of ideal absorbers on the radiated power. However the calculated curves for this model with common absorbers have shown acceptable values with maximum 6-7 dB deviation from the measurements. Therefore, one can dismiss the assumption of weakness of the simplified model in showing the effect of ideal absorbers and instead focus on the reasoning based on the insufficiency of ideal absorbers. This means that even covering the whole surfaces in the engine bay with the best possible absorbers cannot provide more than few decibels reduction in the radiated noise; to achieve a quieter engine bay assembly proper positioning of the absorbers and reducing the openings close to the main radiators are of the same importance as the absorbability of the absorbers.

### 5.3.2. Effect of using ideal absorber on the main absorbers

Here, the ideal absorption property is only given to the main absorbers to see how the radiated sound power is influenced by the high absorption of the main absorbers. To have more precise results, the detailed geometry is used for simulations in this test. Figure 5.8 presents the outcomes of this investigation.

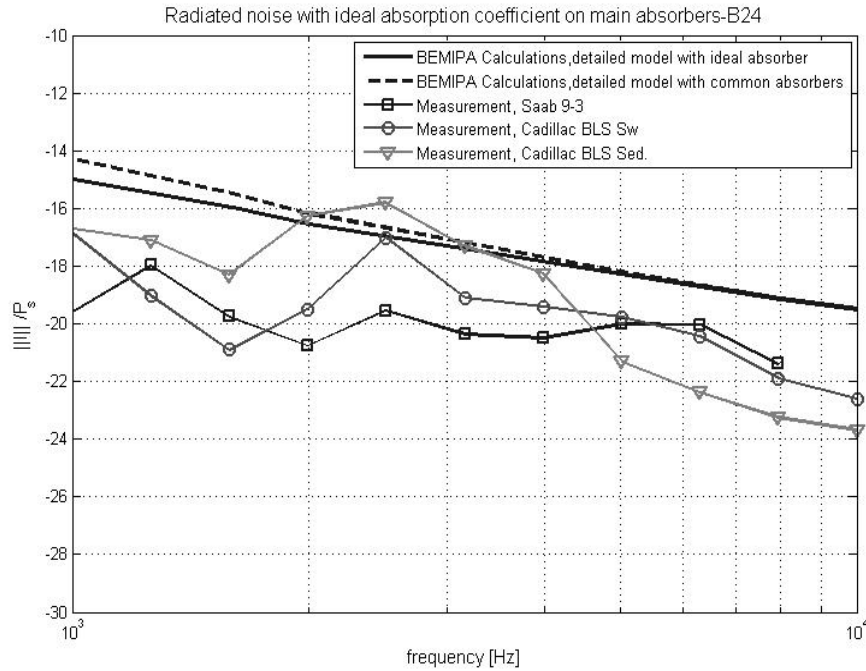


Figure 5.8: Single source B24 - Comparison between radiated sound power when using ideal absorber on the main surfaces with the model with common absorbers and the measured values in the 3 engine bays

As is shown above, the maximum radiation reduction after assigning ideal absorption to the main absorbers is less than 1dB at 1 kHz. The radiation curve for the case of ideal absorber on the main surfaces converges the curve related to the model with common absorbers and above 2 kHz these curves show almost the same values. This implies that even if the best possible absorbers are installed on the main absorbing surfaces, it is not possible to reduce the radiated sound more than very few decibels. Consequently, to obtain higher reductions in the emitted noise from the engine bay, solutions other than increasing the sound absorption of the current absorbers should be figured out.

### 5.3.3. Effect of the equivalent scattering absorbers

All the surfaces except the main absorbers in the CAD models are called equivalent scattering absorbers and are assigned with absorption coefficient values lower than the main absorbers. In order to visualize the effect and importance of the equivalent scattering absorbers, a situation that all of the surfaces inside the engine bay except main absorbers are rigid is compared with the model with common absorbers. In the first model main absorbers are assigned with main absorption coefficient curve. To avoid long calculation times, the simplified geometry including the back part is chosen for this comparison.



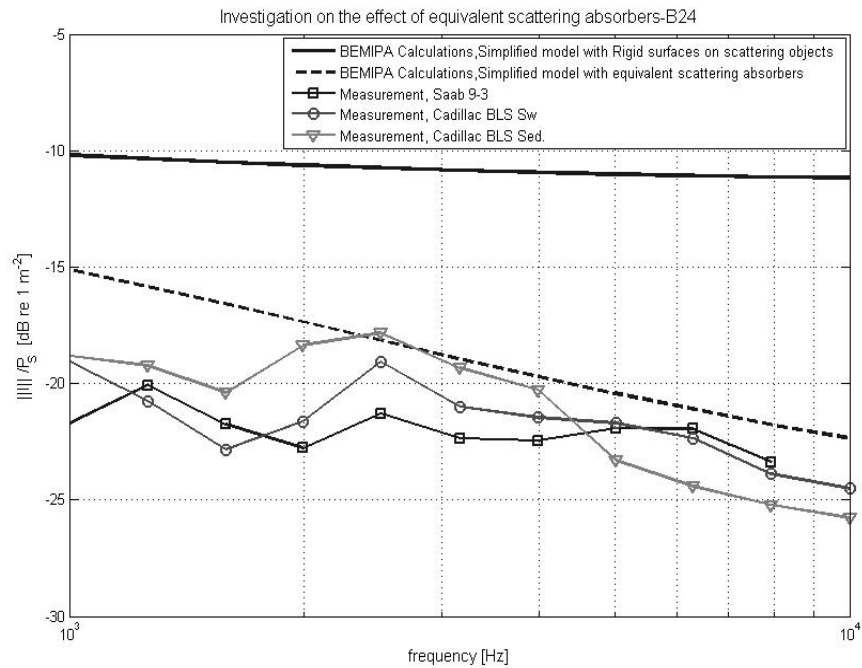


Figure 5.9: Single source B24 - Comparison between radiated sound power when assuming rigid surfaces for the scattering objects and accessory parts in the engine bay with the model with equivalent scattering absorption on these surfaces.

Figure 5.9 shows at least 4 dB higher radiated power for the case that scattering absorbers are replaced with rigid surfaces. Also the difference between these curves and the measured values is at least 8dB at low frequencies and up to 12 dB at highest frequencies. This means that even though the equivalent scattering absorbers are weaker than the main absorbers in absorbing the sound waves, they still play a critical role in reducing the level of radiated power. Therefore, when modelling the sound field due to radiation from the engine bay it is very important to take into account the sound absorbing effects of the parts like wires, cables and other scattering objects even if they are not included in the geometry model. Investigation on the models with common absorbers shows that when equivalent scattering absorbers are included in the model, simulation results are in an acceptable range compared to the measurements. Therefore, one could conclude that the equivalent absorption properties which are used in BEMIPA simulations are satisfying for our engine bay case.

## 6. Results: Prediction of the radiated sound field from an engine bay

### 6.1. Total averaged radiated power from several sources

It was mentioned in section 5.2 that the differences between calculated radiation curves and measurements can be to some extent due to considering the radiation from a single source and this can magnify the effect of some sound absorbing surfaces which are closer to the source. This effect can add directivity to the radiated power while in IPA method for derivation of the boundary condition for the absorbers it is assumed that the incident power is uniformly distributed over all angles of incident which violates the directivity effect. In addition in a real engine bay it is not usually single sources which cause the engine noise, but there are several radiators in a region which emit noise. According to the mentioned reasons, in this section radiated sound powers from groups of at least 6 sources are calculated by modifying BEMIPA to give total radiated power from several sources. These results are compared with superposition of the corresponding sources in the measurements as well as the single source calculations outputs. To relate this part of the results to the previous ones, each group of sources are selected in the vicinity of the four single sources which were used in the previous calculations: A06, B2, B24 and B32. The selected regions are shown in Figure 6.1.

Figure 6.2 illustrates the calculated power curves for each region of the engine bay and compares them with the corresponding curves based on measurements. Calculations are based on the detailed geometry to be closer to reality. To make multiple-source calculation and measurement results comparable with the single-source results, all the curves should have the same total input power. In the single-source investigations the source has unit input power, and to obtain this input power for the multiple-source cases, BEMIPA code can be modified in two ways; either by setting the amplitude of each source as one divided by the number of sources ( $1/\text{number of sources}$ ) or by dividing the final calculated power by the number of sources at each region ( $\frac{\text{total radiated power}}{\text{number of sources}}$ ).

In Figure 6.2 only the measured values taken from Saab 9-3 engine bay are plotted. Since it was the only set of measurements which included radiated power from the sources all over the engine bay. However, since the difference between measured values for the 3 engine bays does not exceed 5 dB at each frequency, it would be

enough to show that the simulations can provide a good prediction of one of the measurement sets.

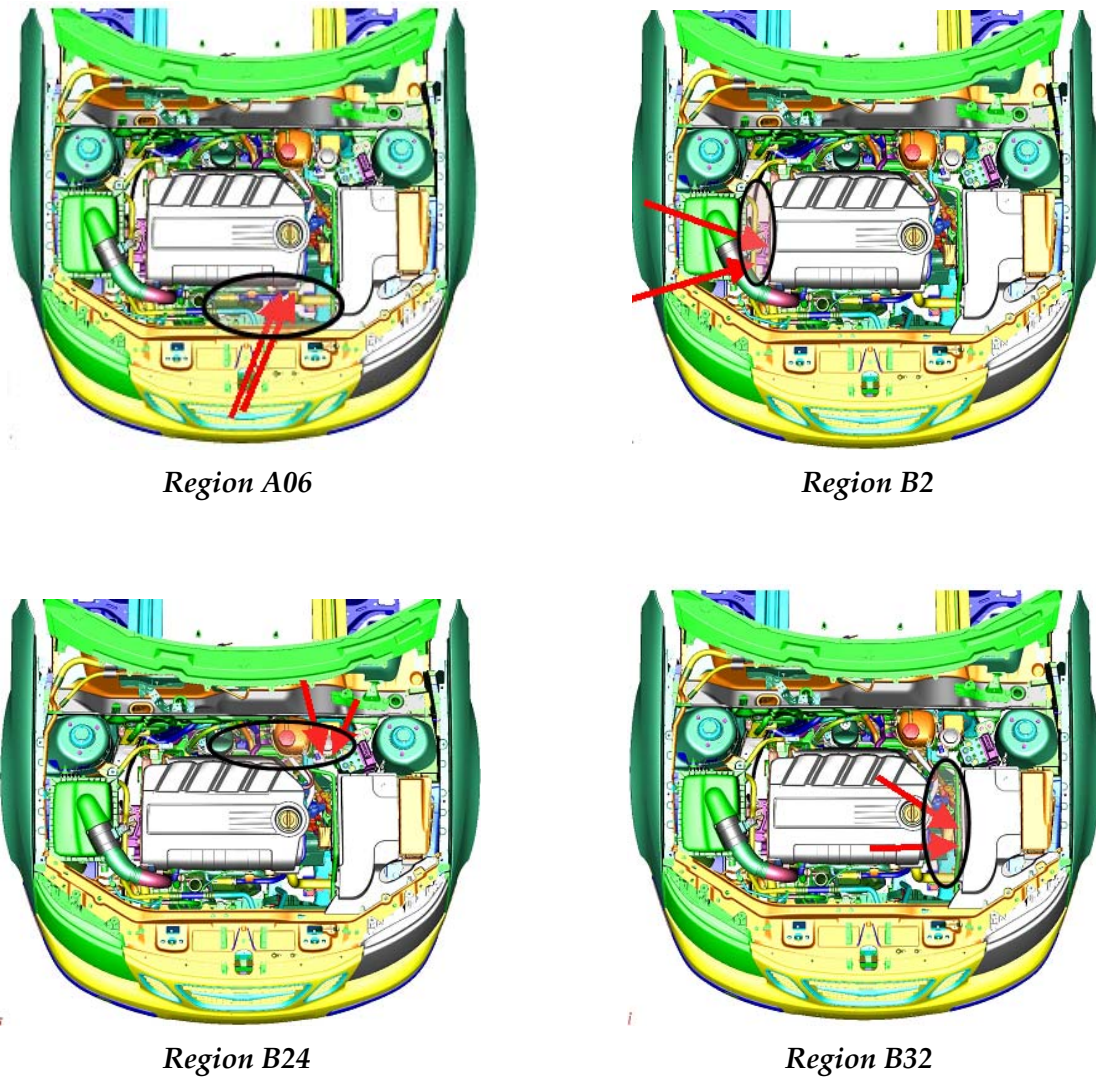


Figure 6.1: The selected regions for calculation of total averaged radiated power from several sources. Each region is marked with a black oval.

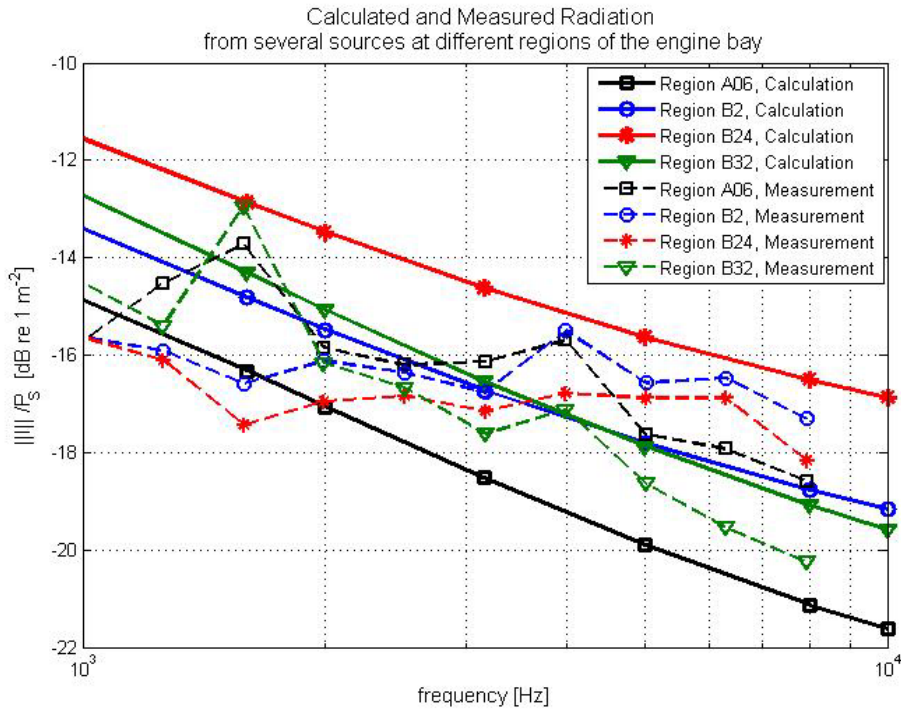


Figure 6.2: Calculated and measured Total Averaged radiated sound power for several point sources in different regions. The total input power to each group of sources is 1 watt. Solid lines are calculated values and dashed lines are measurement results.

The maximum deviation between calculated values and the measurements is 4dB which shows how good the BEMIPA model modified for several sources has been able to predict the radiated sound field. Comparing these results with the single-source calculations, one can conclude that when there are more sources involved in the simulations and the directivity effects are minimized the results will be much closer the real values taken from engine bays.

# 7. Conclusions

## 7.1. Summary

Current thesis is designed to follow different goals concerning sound field prediction at high frequencies (1-10 kHz). Although the thesis is a part of the project "Reduction of external noise for diesel propelled passenger cars" at Saab Automobile AB, it also focuses on evaluating the capabilities of combination of the boundary element method (BEM) and the intensity potential approach (IPA) for modelling sound radiation from a partial enclosure at high frequencies. The enclosure is an engine bay which makes a fairly large domain and is filled with objects of different properties and sizes. These characteristics make prediction of the radiated noise from an engine bay seem a difficult case to study in the beginning, but the final outcomes of the thesis shows that it is not impossible.

To predict the radiated sound power levels from an engine bay, BEMIPA method implemented as a Matlab/Fortran programme developed at Applied Acoustics is used. BEMIPA is an energy-based method which solves the intensity potential equation with the boundary element method to predict sound radiation from sources in a partial enclosure to the surrounding.

In the early steps of the project, to evaluate BEMIPA, the behaviour of the method due to source positioning, different geometrical details and different absorbing properties is investigated. For each case the radiated power from single sources is calculated and the results are compared with the measured values taken from three real engine bay constructions. To study the effect of source positioning, sound power is calculated for four single source positions in different regions of the engine bay. The influence of geometrical details is tested by using three geometrical configurations of the engine bay in the simulations. These configurations consist of two simplified geometries lacking many objects and accessory parts and a more detailed geometry which is not as detailed as a real engine bay but includes some more engine walls and surfaces compared to the simplified models. In the last step of the method evaluation, the effect of sound absorbing surfaces is investigated by trying different configurations of absorbers on the surfaces of the engine bay.

Once the strengths and weaknesses of the BEMIPA method in prediction of the radiated sound field are realized, the method is applied to calculate the radiated power from the engine bay for more realistic cases when several sources in a region contribute to the radiated field. To confirm the competence of the method in prediction of a realistic sound field, the calculation results are then compared with

measured total averaged radiated energy taken from the corresponding sources in different regions of the real engine bays.

## 7.2. Outcome of the thesis

Radiated sound power levels calculated by BEMIPA method demonstrate a very good agreement with the measured values taken from the real engine bays. Although the geometry models applied in the calculations are simplified and do not include many details of the real engine bays, the difference between calculations and measurements does not exceed 5dB on average. Maximum 5dB deviation (on average) between measurements and calculations becomes more acceptable when mentioning that even between the measurement curves belonging to the three engine bays of similar construction, there is up to 4dB deviation at each frequency. This can be due to the high sensitivity of the measurements to the positioning of microphones.

When BEMIPA calculations are performed under more realistic conditions with several single sources radiating at the same time in each region, the competency of the method in prediction of the sound field becomes even clearer compared to the cases that radiation from only single sources is considered. The reason is embedded in the boundary conditions of the IPA method for sound absorbers. The assumption behind these boundary conditions is that the sound waves hit the surface from several directions and the incident power is uniformly distributed over the angle of incidence. This condition is closer to the case when several sources at different positions of a region radiate sound rather than the single source calculations.

Simplification of the geometry models which aims to reduce the complexity and the time of calculations underestimates the scattering effect of many accessory parts which are missing from the engine bay models. These sound scattering objects can effectively increase the total absorption of the engine bay and play an important role in reduction of the total radiated sound level in reality. As is suggested in [7] and [8] the sound scattering effect of the missing objects can be compensated by adding extra equivalent absorption to different surfaces. The close proximity of the calculated curves to the measurements proves that this approach is a proper solution for taking the effect of these scatterers into account.

Investigations on the simplified and detailed geometrical models showed that at high frequencies, position of the absorbers and the openings of the system relative to the noise sources are the most determining factors in simulation of the sound field, while the small geometrical details between the models do not have any distinctive influence on the results.

Examinations on the effects of absorbers in the simulation results illustrated that even if all the surfaces inside the engine bay are covered with ideal absorbers, it would not be possible to achieve more than 8 dB reduction at lowest frequencies and 2dB at highest frequencies. Therefore, if high reduction of noise levels are of interest it is better to concentrate on changing the geometry by for example reducing the openings of the engine bay rather than increasing the absorption of the surfaces.

Although the BEMIPA method provides satisfactory simulation results compared to the real measurements, there are still slight differences between them. These differences can be due to uncertainties in the geometrical models, coordinates of the sources and the boundary conditions, limited number of receivers used in the simulations, insufficiency of the equivalent scattering absorbers to model the effect of scattering objects and etc. However, achieving maximum 5 dB difference between calculations and measurements proves that these limitations have not prevented BEMIPA method from predicting the high-frequency sound field competently. Comparing the simulation and measurement results shows that as long as we are interested in the trend of radiation, averaged levels of radiated sound power and extent of radiation from different regions of the engine bay, BEMIPA method can be a pretty well solution.

### 7.3. Future work

A suggestion for future work is to use BEMIPA to identify those regions of the engine bay which leak noise and have higher radiated sound levels compared to the other regions.

Further investigations can also be conducted on the real engine noise properties. The source data of the engine noise can be inserted to the BEMIPA code which is modified for the new source conditions and consequently the simulation results would get even closer to the real radiated sound field.

Based on the identified weakness points of the engine bay and the realistic radiated sound field, the investigations can be extended to come up with proper geometrical changes in the engine bay design that can control the escape ways of the engine noise and reduce the radiated sound power from the engine bay.

# Bibliography

- [1] <http://europa.eu/>
- [2] Andersson, P.B.U. and Lindberg, E., *Boundary element method for intensity potential for prediction of sound power radiation at high frequencies*, Journal of the Acoustical Society of America, submitted, 2009
- [3] Thivant, M., Andersson, P.B.U. and Guyader, J L, *Intensity potential approach for modeling high-frequency sound fields*, Journal of the Acoustical Society of America, submitted, 2009
- [4] Andersson, P.B.U., *Solving the intensity potential problem by using the boundary element method*, In Proceedings of InterNoise2010, Lisbon, Portugal, 2010
- [5] Pascal, J.-C. and Li, J.-F., *Irrotational acoustic intensity: A new method for location of sound sources*, sixth international congress on sound and vibration, Copenhagen, Denmark, 1999
- [6] Andersson, P., *Characterisation of acoustical properties of engine bays by using measured FRFs*, Report S08:05, Div. of Applied Acoustics, Chalmers University of Technology, Göteborg, Sweden, 2008
- [7] Atak, O., *Evaluation of Boundary Element Method as a tool in analysis of acoustical performance of absorber and screen systems in engine bays*, Master thesis, Chalmers university of technology, Gothenburg, Sweden, 2009
- [8] Lindberg, E. and Andersson, P.B.U., *Experimental investigation of sound power radiation from partly open enclosure with numerous interior objects*, 19<sup>th</sup> international Congress on Acoustics, Madrid, Spain, 2007
- [9] Möbius, F., *Characteristics and functioning of membrane absorbers covered with micro-perforated panels*, Gothenburg, Sweden, 2007
- [10] Schönfeld, S., *Airborne sound transmission loss of a car firewall: Prediction and study using Statistical Energy Analysis*, Master thesis, Chalmers university of technology, Gothenburg, Sweden, 2008
- [11] Corakci, A., Tober, S., *Modeling of interior sound field in railway vehicles: Special focus on sound transmission between vestibules and saloons*, Master thesis, Chalmers university of technology, Gothenburg, Sweden, 2009



# Appendix A

## A.1. Simplified model without the back part

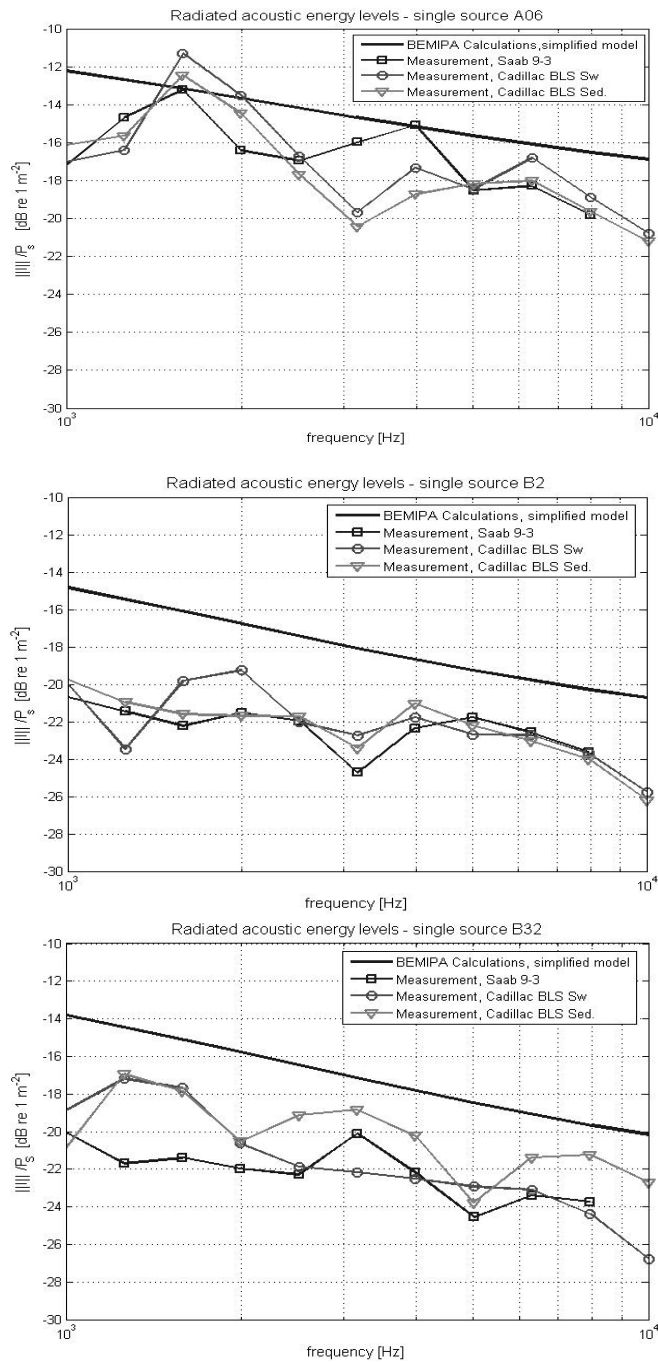


Figure A.1: Calculated values are based on *simplified model without the back part* and measurements are performed on three engine bays with similar construction but difference in details.

## A.2.Effect of the back part

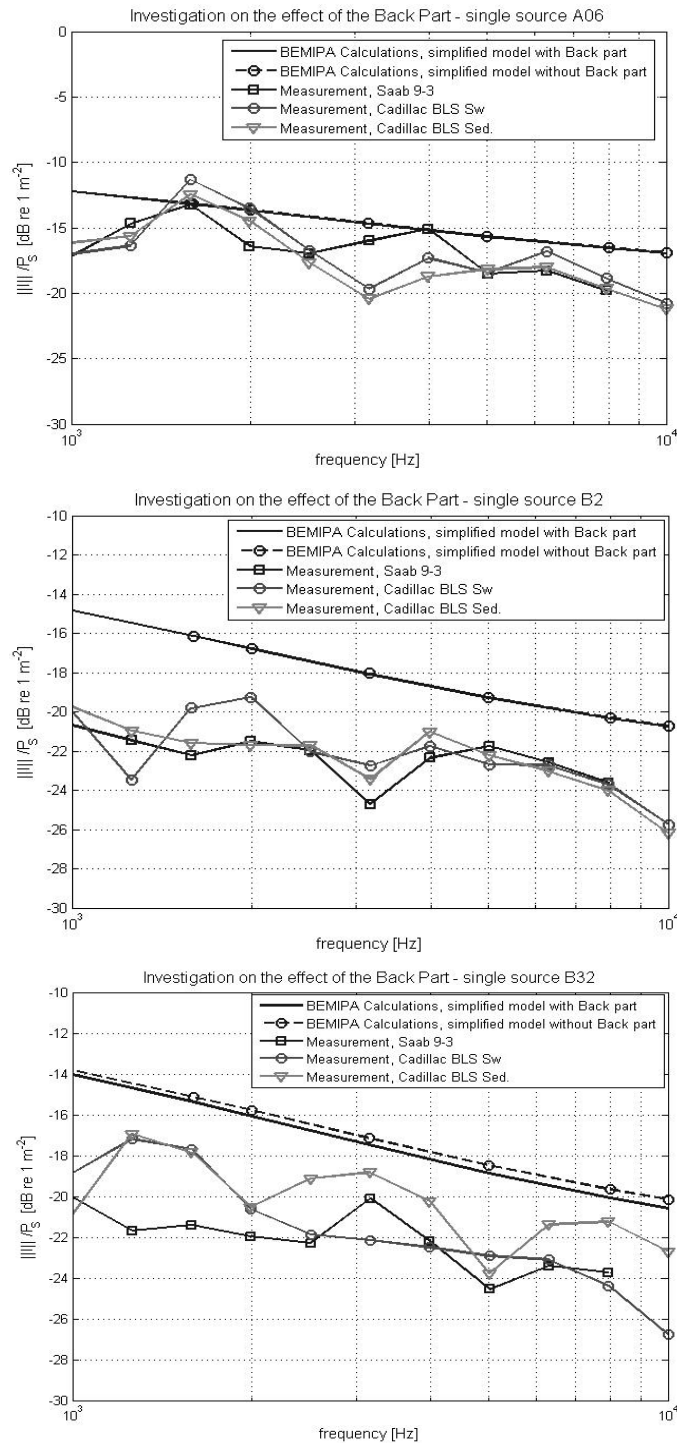


Figure A.2: Calculated values are based on the two *simplified models with and without the back part* and measurements are performed on three engine bays with similar construction but difference in details.

### A.3. Detailed model calculations

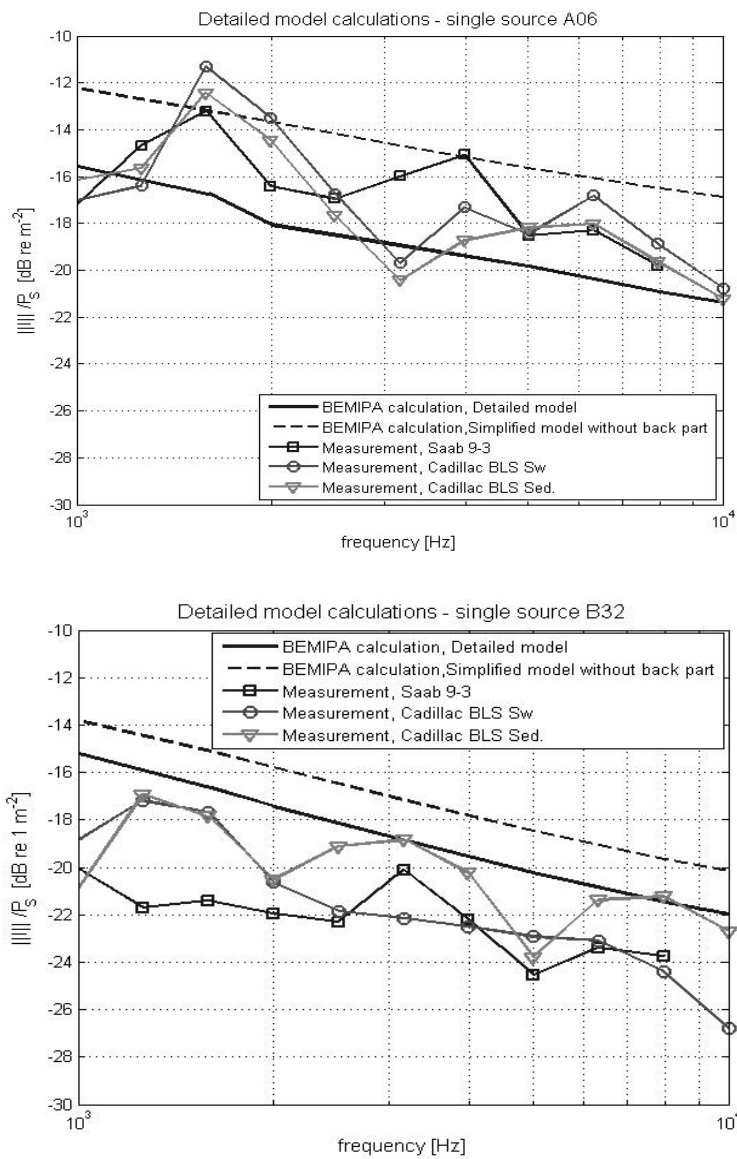


Figure A.3: Calculated values are based on *detailed model* and *simplified model without the back part* and measurements are performed on three engine bays with similar construction but difference in details.

## A.4. Effect of ideal absorber on all surfaces

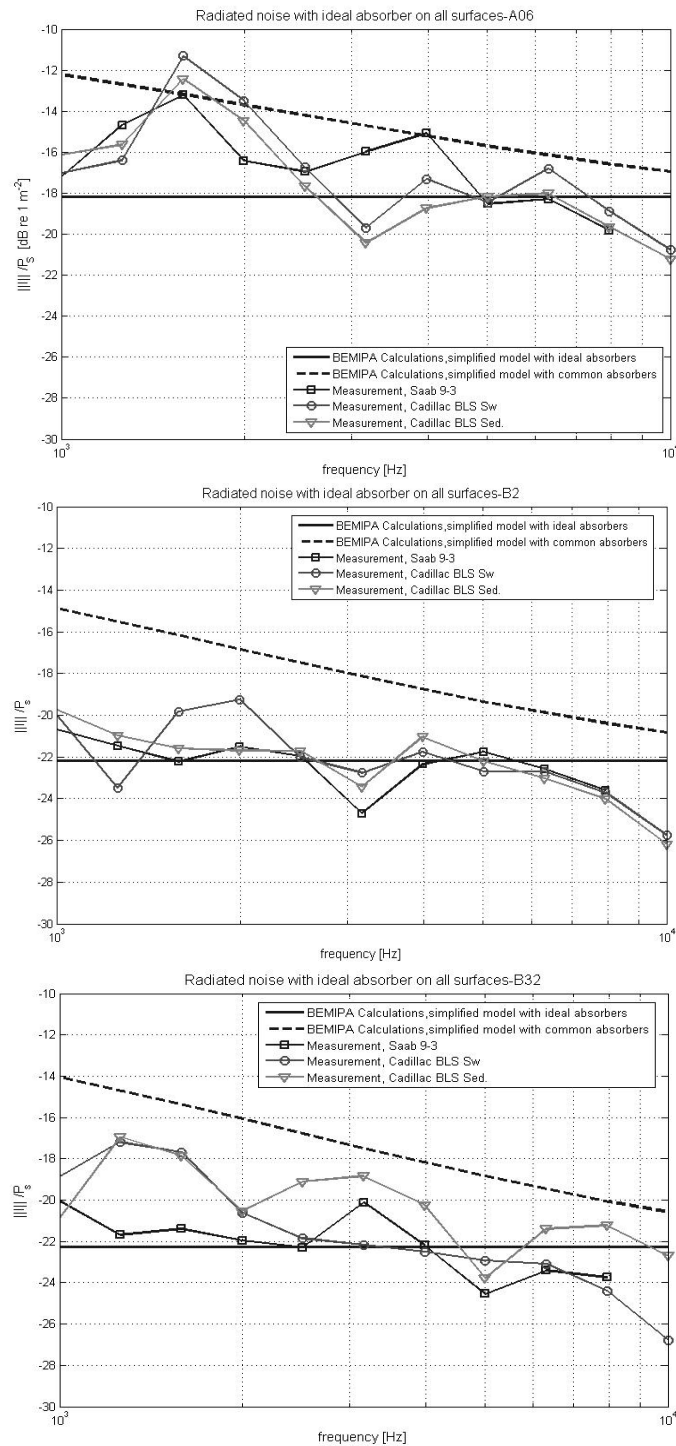


Figure A.4: Calculated values are based on *simplified model including the back part* for two situations: 1-The surfaces are assigned with Main and Equivalent scattering absorption properties 2- All surfaces are assigned with ideal absorption.

## A.5. Effect of using ideal absorber on the main absorbers

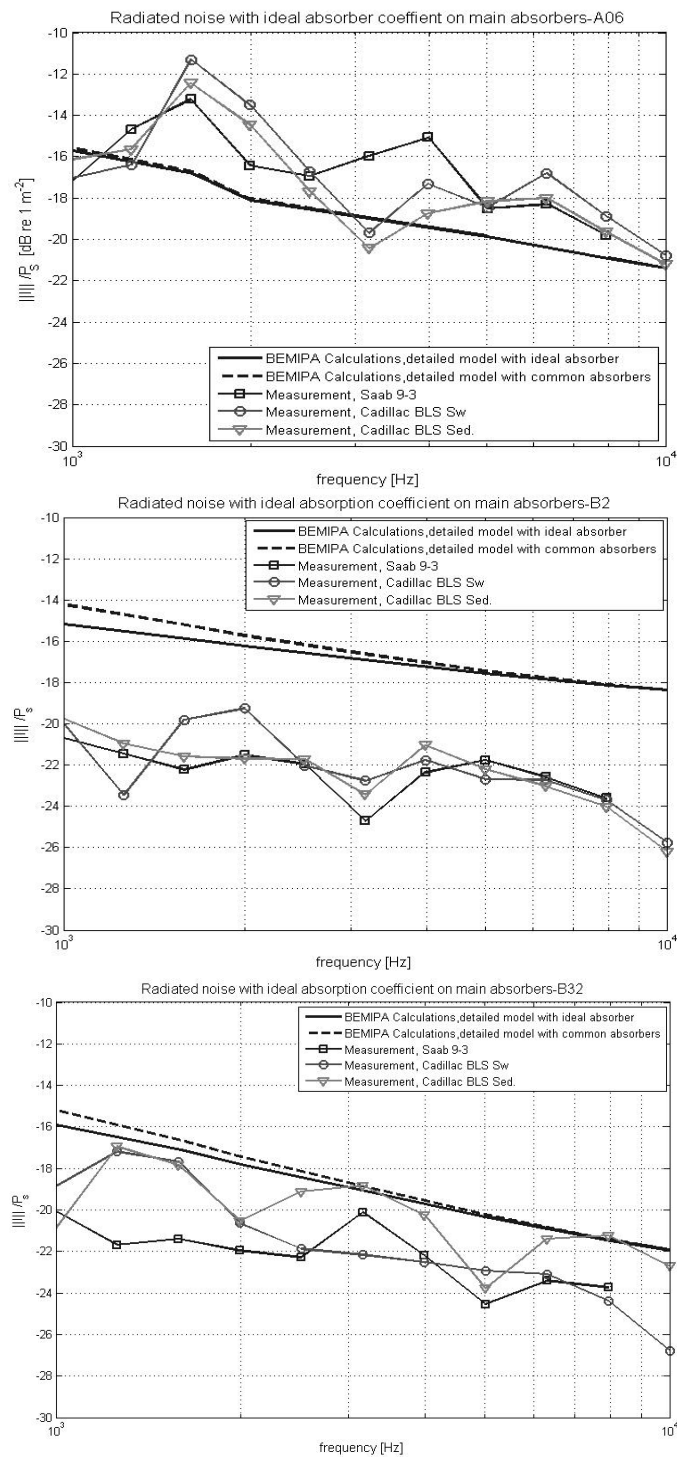


Figure 0.5: Comparison between radiated sound power when using ideal absorber on the main surfaces with the model with common absorbers and the measured values in the 3 engine bays

## A.6. Effect of equivalent scattering absorbers

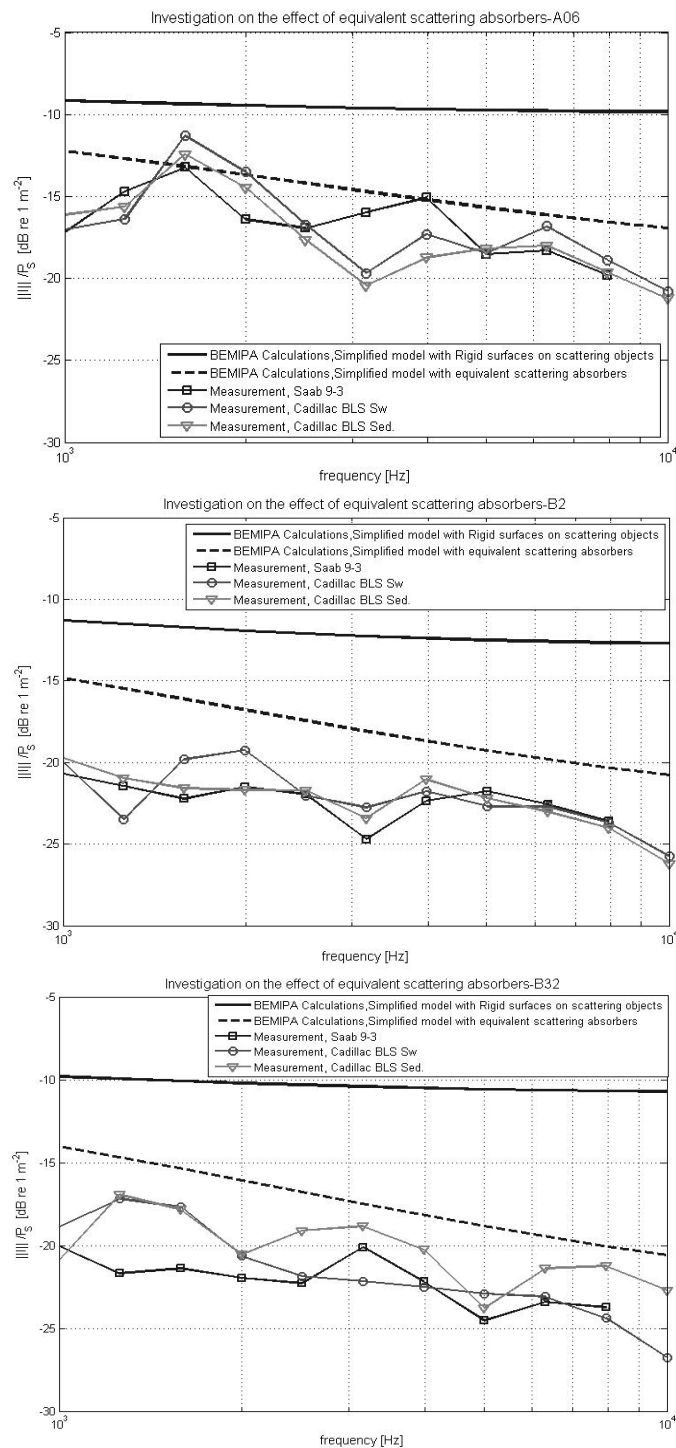


Figure 0A.6: Comparison between radiated sound power when assuming rigid surfaces for the scattering objects and accessory parts in the engine bay with the model with equivalent scattering absorption on these surfaces.

# Appendix B

## Radiated power from sources close to absorbers

From the calculations results during the project, it became clear that position of the source relative to the absorbing surface is a determining factor in the radiated sound power from the engine bay. To validate this dependence a set of tests were performed on a simple model of a monopole source on top of an absorbing plate with the same absorption coefficient curve as the main absorbers in the engine bay simulations. The investigation was done for different distances between source and the plate. The resulting radiation curves are presented in Figure B.1.

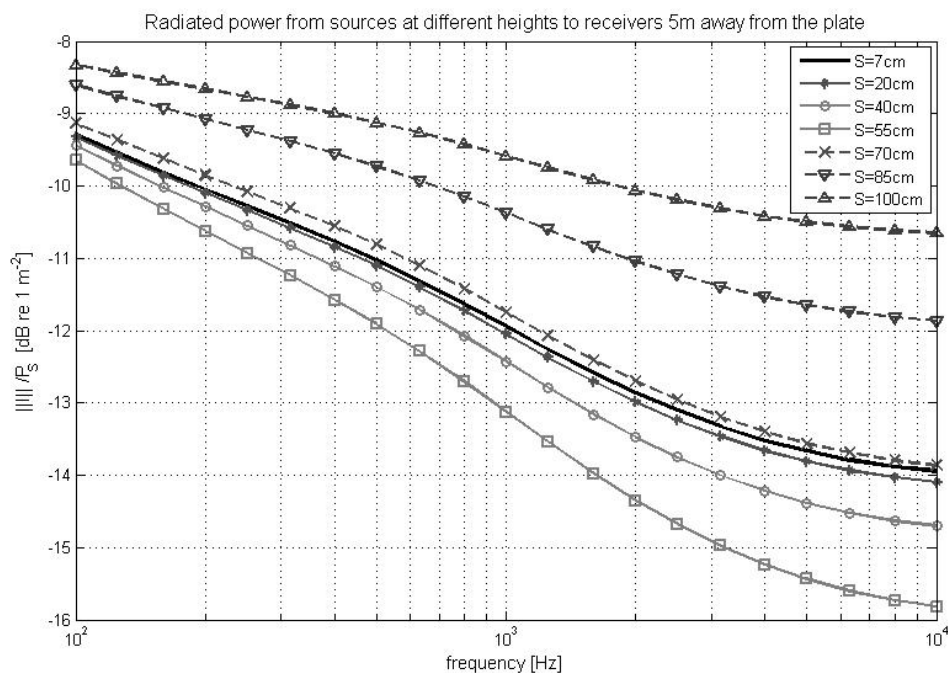


Figure B.1: Radiation from a point source at different distances on top of an absorbing plate having dimensions of  $3 \times 4.5 \times 0.075$  m $\times$ m $\times$ m.

The distances between monopole source and the plate are selected in a way that they resemble the real possible distances in the engine bay and in the CAD models.

Figure B.1 illustrates that when the source is very close to the plate, by increasing the distance, absorber acts more effectively and the radiated sound to the receivers decreases. The reduction increases with the distance until it reaches to an optimum distance. After this point, by increasing the distance the radiation increases accordingly. To explain this trend the analysis should be divided into two parts; first,

the decrease of radiated power by increasing the distance between source and the plate should be discussed. In the second part the reason for the increase of radiated levels after a specific distance should be investigated.

For the first part of analysis one could say that when the source is very close to the surface the absorber cannot work effectively due to the grazing incidence effect. By increasing the distance between source and the absorbing plate, a larger part of the surface can be exposed to the sound waves and more waves have the chance to hit the surface with a proper angle to penetrate into the absorber. According to the reflection coefficient formula presented in (2.21) the bigger  $Z\cos\varphi$  is, the smaller reflection coefficient will be and consequently the surface absorption will be higher. At small distances between source and the absorber, increasing the distance causes  $\varphi$  angle become smaller, so  $Z\cos\varphi$  gets larger and the absorber acts more effectively and radiated sound decreases. However, after an optimum distance between the source and absorber which results in maximum sound absorption, the radiation becomes less dependent on the reflection factor and absorption coefficient of the surface. In our case this happens for source positions farther than 50 cm from center of the plate. After this point the solid angle between the source and the plate becomes of more importance. This leads to the second part of the analysis to explain how the radiated sound varies based on the solid angle.

Based on the definition solid angle is a three-dimensional angle, formed by three or more planes intersecting at a common point. In here the common point is the source and intersecting planes are the four planes made by connecting each 2 corners of the plate to the source, so by taking the source farther from the plate this angle becomes smaller. Solid angle represents the extent of visibility of an object from a specific point or to relate it to our acoustic problem one could say that only the portion of sound waves which propagate inside the arms of solid angle would hit the surface of absorbers and have the chance of being absorbed by the absorber. When the source gets farther from the plate, the solid angle becomes smaller meaning that a smaller portion of the sound waves radiating in a spherical shape from the point source hit the surface and consequently a larger portion can reach to the receivers without being affected by the absorber. This leads to a higher level of radiated power.